A 135,000-year Vostok-Specmap Common temporal framework

Todd Sowers, Michael Bender, Laurent Labeyrie, Doug Martinson, Jean Jouzel, Dominique Raynaud, Jean Jacques Pichon, Yevgeniy Sergeevich Korotkevich

PALEOCEANOGRAPHY, VOL. 8, NO. 6, PAGES 737-766, DECEMBER 1993

A 135,000-YEAR VOSTOK-SPECMAP COMMON TEMPORAL FRAMEWORK

Todd Sowers,[1] Michael Bender,[1,2]
Laurent Labeyrie,[2] Doug Martinson,[3]
Jean Jouzel,[4,5] Dominique Raynaud,[6]
Jean Jacques Pichon,[7] and
Yevgeniy Sergeevich Korotkevich[8]

Abstract. The object of the present study is to introduce a means of comparing the Vostok and marine chronologies. Our strategy has been to use the $\delta^{18}O$ of atmospheric O_2 (denoted $\delta^{18}O_{atm}$) from the Vostok ice core as a proxy for the $\delta^{18}O$ of seawater (denoted $\delta^{18}O_{sw}$). Our underlying premise in using $\delta^{18}O_{atm}$ as a proxy for $\delta^{18}O_{sw}$ is that past variations in $\delta^{18}O_{sw}$ (an indicator of continental ice volume) have been transmitted to the atmospheric O_2 reservoir by photosynthesizing organisms in the surface waters of the world's oceans. We compare our record of $\delta^{18}O_{atm}$ to the $\delta^{18}O_{sw}$ record which has been developed from studies of the isotopic composition of biogenic calcite ($\delta^{18}O_{foram}$) in deep-sea cores. We have tied our $\delta^{18}O_{atm}$ record from Vostok to the SPECMAP timescale throughout the last 135 kyr by correlating $\delta^{18}O_{atm}$ with a $\delta^{18}O_{sw}$ record from V19-30. Results of the correlation indicate that 77% of the variance is shared between these two records. We observed differences between the $\delta^{18}O_{atm}$ and the $\delta^{18}O_{sw}$ records during the coldest periods, which indicate that there have been subtle changes in the factors which regulate $\delta^{18}O_{atm}$ other than $\delta^{18}O_{sw}$. Our use of $\delta^{18}O_{atm}$ as a proxy for $\delta^{18}O_{sw}$ must therefore be considered tentative, especially during these periods. By correlating $\delta^{18}O_{atm}$ with $\delta^{18}O_{sw}$, we provide a common temporal framework for comparing phase relationships between atmospheric records (from ice cores) and oceanographic records constructed from deep-sea cores. Our correlated age-depth relation for the Vostok core should not be considered an absolute Vostok timescale. We consider it to be the preferred timescale for comparing Vostok climate records with marine climate records which have been placed on the SPECMAP timescale. We have examined the fidelity of this common temporal framework by comparing sea surface temperature (SST) records from sediment cores with an Antarctic temperature record from the Vostok ice core. We have demonstrated that when the southern ocean SST and Antarctic temperature records are compared on this common temporal framework, they show a high degree of similarity. We interpret this result as supporting our use of the common temporal framework for comparing other climate records from

[1]Graduate School of Oceanography, University of Rhode Island, Narragansett.
[2]Centre des Faibles Radioactivites, Laboratorie Mixte CNRS-CEA, Gif Sur Yvette, France.
[3]Lamont-Doherty Earth Observatory Palisades, New York.
[4]Laboratoire de Modelisation du Climat et de l'Environnement, Gif Sur Yvette Cedex, France.
[5]Also at Laboratoire de Glaciologie et Geophysique de l'Environnement, St. Martin d'Heres Cedex, France.
[6]Laboratoire de Glaciologie et Geophysique de l'Environnement, St. Martin d'Heres Cedex, France.
[7]Department Géologie et Océanologie, Université Bordeaux, Talence Cedex France.
[8]Arctic and Antarctic Research Institute, St. Petersburg, Russia.

Paper number 93PA02328.
0883-8305/93/93PA-02328$10.00

the Vostok ice core with any climate record that has been correlated into the SPECMAP chronology.

INTRODUCTION

Studies of ice cores have supplied vast amounts of information about late Pleistocene climate. Variations in the isotopic composition of the ice from Greenland and Antarctic ice cores have been used to construct temperature records for these sites [Dansgaard et al., 1985; Lorius et al., 1985; Hammer et al., 1986; Jouzel et al., 1987; Johnsen et al., 1992]. Other important records which have been constructed from ice core analyses include the composition of the paleoatmosphere [Neftel et al., 1988; Raynaud et al., 1988; Stauffer et al., 1988; Chappellaz et al., 1990; Barnola et al., 1991; Etheridge et al., 1992] and a record of aerosol transport to the ice sheets [Raisbeck et al., 1987; Petit et al., 1990].

The original chronology for the Vostok ice core was constructed using a two-dimensional rheologic model of the ice flow upstream from Vostok in conjunction with a record of the paleoaccumulation rate [Lorius et al., 1985]. The chronology for the trapped air parcels was derived by calculating a record of the ice age-gas age difference (Δage) [Barnola et al., 1987,1991] and subtracting it from the ice age versus depth relation of Lorius et al. [1985]. The approach adopted here is to correlate our record of the $\delta^{18}O$ of atmospheric O_2 ($\delta^{18}O_{atm}$) from Vostok with the $\delta^{18}O$ of seawater ($\delta^{18}O_{sw}$) derived from studies of the $\delta^{18}O$ of foraminiferal calcite. Our underlying premise in using $\delta^{18}O_{atm}$ as a proxy for $\delta^{18}O_{sw}$ is that past variations in $\delta^{18}O_{sw}$ have been transmitted to the atmospheric O_2 reservoir by photosynthesizing organisms in the surface waters of the world's oceans. We compare our record of $\delta^{18}O_{atm}$ to the $\delta^{18}O_{sw}$ record which has been developed from studies of the isotopic composition of biogenic calcite of benthic foraminifera ($\delta^{18}O_{foram}$) in deep-sea cores [Labeyrie et al., 1987; Shackleton, 1987]. In making such a correlation we derive a direct estimate of a gas age versus depth relation for Vostok that is consistent with the marine chronostratigraphy. Our correlation provides the basis for a more direct comparison of the atmospheric pCO_2 and pCH_4 records from Vostok with climate records obtained from deep-sea sediment studies covering the last 140 kyr.

ICE CORE AND DEEP-SEA CORE CHRONOSTRATIGRAPHIES

Deep-Sea Chronostratigraphies

Most records of Pleistocene climate constructed from deep-sea cores can be placed into one of the two SPECMAP timescales (the lower-resolution long timescale [Imbrie et al., 1984] or the higher-resolution short timescale [Martinson et al., 1987]). The stratigraphic bases for these timescales are the SPECMAP stacked $\delta^{18}O_{foram}$ records (long record [Prell et al., 1986] and short record [Pisias et al., 1984]) which allow direct transfer of the timescales through correlation with any other $\delta^{18}O_{foram}$ versus age records. The basis for these two SPECMAP chronologies is that variations in the Earth's orbital geometry influence incoming solar radiation which in turn forces, or at least paces, variations in the size of the continental ice sheets [Hays et al., 1976*a*; Imbrie et al., 1984]. The higher-resolution short SPECMAP chronology (used here) was constructed using four different "tuning" strategies involving five proxy climate indicators (including the $\delta^{18}O_{foram}$ record) from RC11-120 [Hays et al., 1976*a,b*] (Figure 1) as well as the SPECMAP stacked $\delta^{18}O_{foram}$ record [Pisias et al., 1984]. Errors in this timescale, estimated using various climate indicators, deep sea cores, and tuning strategies, average ±3.5 kyr and range from 1 to 7 kyr. The short SPECMAP timescale has also served as the basis for correlating other records such as the China loess deposits [Kukla and An, 1989; Hovan et al., 1991] and pollen records from North America and Europe [Guiot et al., 1989].

Ice Core Chronostratigraphies

Dating ice cores retrieved from the East Antarctic plateau has proven difficult because of the lack of annual stratigraphic layers in the ice. Lorius et al. [1985] established a timescale for the Vostok ice core with the use of a two-dimensional ice flow model. Their approach utilized a record of the paleoaccumulation rate in conjunction with model calculations of the degree to which annual layers have been thinned during transport within the East Antarctic ice sheet (commonly referred to as the thinning function). Recent sensitivity studies suggest that an ice age-depth profile for an ice core is largely dependent on the paleoaccumulation record used [Ritz, 1992]. The original Vostok chronology was constructed by assuming that the accumulation rate upstream from Vostok was directly related to the δD or $\delta^{18}O$ of the precipitation. This assumption was later supported by ^{10}Be measurements [Yiou et al., 1985; Raisbeck et al., 1987; Jouzel et al., 1989; Raisbeck et al., 1992]. On the other hand, the average δD_{ice} from the Dome B core (located ~300 km upstream from Vostok) during the Holocene is 7‰ higher than that for the Holocene section of the Vostok ice core [Kotlyakov, 1990]. The end of the last glacial-interglacial transition (~10 ka) is about 140 m deeper at Dome B than at Vostok. The inferred accumulation rate at Dome B over this period is thus 60% higher than at Vostok. This result is much higher than the 10% difference which would be derived from the difference between the δD_{ice}

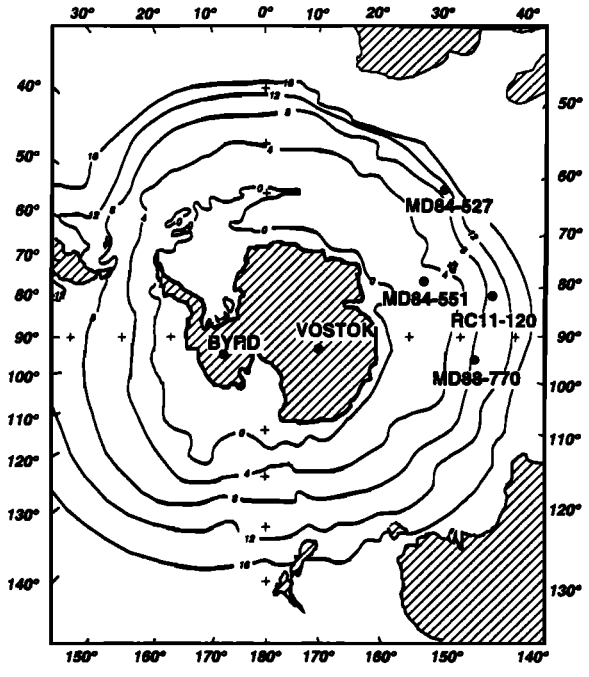

Fig. 1. Index map showing the location of the deep-sea sediment core (MD88-770, 46°S, 96°E) as well as the Antarctic ice cores included in our study. Also plotted are the summer sea surface temperature isotherms for the southern ocean.

values of the ice at the two sites. Ritz [1992] concluded from this observation that the accumulation rate near Vostok is not solely controlled by the temperature of the inversion layer. Other factors, such as the orographic and radiative cooling appear to significantly influence the accumulation rate over East Antarctica (C. Ritz, Chronology of the Vostok ice core based on precipitation and ice flow modeling, submitted to *Journal of Glaciology*, 1993). Furthermore, Jouzel et al. [1992] showed that, when the same glaciological model was applied to both the Vostok and Dome C cores, the timing of the minimum in the dust flux near the beginning of the last glacial termination at the two sites was different by about 1 kyr. These results have been incorporated into a revised flow model for the Vostok area which now extends to 2546 meters below the surface [Jouzel et al., 1993].

Minor modifications to the Lorius et al. [1985] Vostok chronology were proposed in three later studies. Jouzel et al. [1987] used a more detailed δD_{ice} record in place of the $\delta^{18}O_{ice}$ record for estimating the inversion layer temperature above Vostok and the paleoaccumulation rate. They recalculated the Vostok age-depth curve based on the revised paleoaccumulation rates and found that the revised chronology agreed well with that of Lorius et al. [1985]. Petit et al. [1990] correlated the Vostok dust record with the magnetic susceptibility record from RC11-120 (taken to be a dust proxy). They suggested that the Lorius et al. [1985] age for the marine stage 5e was about 10 kyr older than the SPECMAP age, and noted that $^{230}Th/^{234}U$ dating studies of corals favored the SPECMAP age [Bard et al., 1990b] (but see Lambeck and Nakada [1992] for another view). Finally, Pichon et al. [1992] compared a record of sea surface temperature (SST) from the southern ocean with the Vostok temperature record to derive a new age-depth curve for Vostok. Pichon et al. [1992] also suggested that the Lorius et al. [1985] age for stage 5e was about 6 kyr older than the corresponding SPECMAP age.

The net result of these correlation studies is to propose various ice age-depth profiles for Vostok which are generally within the stated uncertainties of the original Lorius et al. [1985] chronology. The present work provides another method of correlating the Vostok and marine timescales. We emphasize that the goal of recent correlation studies by Petit et al. [1990], Shackleton et al. [1992], and Pichon et al. [1992] has been to place the Vostok climate records into the SPECMAP chronology. None of the correlation studies gives any indication about which absolute chronology is superior. In the next section we use our record of $\delta^{18}O_{atm}$ to correlate the Vostok and SPECMAP timescales. We focus on developing a common timescale which is suitable for comparing the Vostok and marine climate records. The results from this study have no bearing on the absolute nature of the Vostok timescale itself. Finally, we compare our correlation results with previous correlations and discuss the implications for leads and lags within the climate system.

COMPARING THE $\delta^{18}O$ OF ATMOSPHERIC O_2 WITH THE $\delta^{18}O$ OF SEAWATER

A Record of the $\delta^{18}O$ of SeaWater

We have constructed a record of $\delta^{18}O_{sw}$ from the benthic $\delta^{18}O_{foram}$ record (*Uvigerina senticosa*) from V19-30 (3°21'S, 83°21'W, 3091-m water depth) [Shackleton and Pisias, 1985]. We chose the V19-30 core for two reasons. First, the $\delta^{18}O_{foram}$ record from this core was used in constructing the SPECMAP stacked record [Pisias et al., 1984]. Consequently, the SPECMAP age model was directly applied to this core during the development of the chronostratigraphy. Second, the long $\delta^{18}O_{foram}$ record (>300 kyr) from this core provides a target curve for correlating $\delta^{18}O_{atm}$ variations from deeper (yet to be drilled) sections of the Vostok core into the SPECMAP timescale. We have normalized the $\delta^{18}O_{foram}$ values by arbitrarily removing 3.46‰ from all samples, so that the average Holocene $\delta^{18}O_{foram}$ value is 0‰.

There are two factors which influence the foraminiferal $\delta^{18}O$ record itself. The first is the

$\delta^{18}O_{sw}$, and the second is bottom-water temperature. To correct for bottom-water temperature changes, we have made the following assumptions: (1) glacial bottom waters were 1.7°C colder than interglacial temperatures [Chappell and Shackleton, 1986; Birchfield, 1987; Shackleton, 1987], (2) deep waters warmed during the terminations themselves and cooled during the transition from the last interglacial (stage 5e) to the glacial period (stage 5d), starting at about 120 ka in the SPECMAP chronology [Fairbanks and Matthews, 1978; Labeyrie et al., 1987; Shackleton, 1987], and (3) the temperature change occurred over a 5-kyr period centered within the terminations or 5e-5d boundary. To correct for these temperature variations, we subtract 0.4‰ from all glacial $\delta^{18}O_{foram}$ data [Shackleton and Opdyke, 1973] and apply the correction gradually over the 5-kyr transition periods. The exact timing of the deepwater temperature changes within a transition is difficult to assess on a global scale. Given that the average length of the last two terminations is 10-12 kyr, our placement of the temperature changes in the middle of the transitions introduces a 1-3 kyr uncertainty in the exact timing of the changes in deepwater temperature. This uncertainty is one limit on the accuracy of our common temporal framework for these periods.

A Record of the $\delta^{18}O$ of Atmospheric O_2 From the Vostok Ice Core

We have measured the isotopic composition of trapped O_2 and N_2 from 95 discrete depths along the Vostok 3Γ (2083 m) and BH-1 (178 m) cores. Fossil air samples were extracted from 12- to 16-g ice samples by allowing the ice samples to melt in-vacuo. The ~1-cm^3 (STP) air sample was then quantitatively transferred to a stainless steel sample tube immersed in liquid helium. The air sample was then either equilibrated into a glass ampoule and sealed for later analysis or introduced directly into the sample reservoir of a Finnigan MAT 251 isotope ratio mass spectrometer where it was analyzed against an aliquot of dry air [Sowers et al., 1989, 1991]. We report our results using the delta notation, where the reference is the present day air:

$$\delta^{18}O_{O_2\,ice}=\left\{\left[\frac{^{18}O^{16}O/^{16}O_2\,(sa)}{^{18}O^{16}O/^{16}O_2\,(air)}\right]-1\right\}10^3 \qquad (1)$$

Results of the $\delta^{15}N$ of trapped N_2 ($\delta^{15}N_{N_2\,ice}$) and $\delta^{18}O$ of trapped O_2 ($\delta^{18}O_{O_2\,ice}$) are reported in Table 1. The $\delta^{15}N_{N_2\,ice}$ results are used to correct the $\delta^{18}O_{O_2\,ice}$ values for gravitational fractionation of air in the firn prior to occlusion [Craig et al., 1988; Schwander, 1989; Sowers et al., 1989] according to the following equation:

$$\delta^{18}O_{atm} = \delta^{18}O_{O_2\,ice} - 2(\delta^{15}N_{N_2\,ice}) \qquad (2)$$

Results are listed in Table 1.

We sampled the Vostok 3Γ core roughly every 25 m starting at 140 m below the surface (mbs) and continuing down to 2058 mbs. Given an age of 160 ka for the bottom (2083 mbs) of the 3Γ core [Lorius et al., 1985], our sampling frequency for the deep core corresponds roughly to one sample every 2,000 years. This value is comparable to the current turnover time of atmospheric O_2 [Bender et al., 1985]. In addition to sampling every 25 m, we performed high-resolution sampling during periods of major climate change. On the other hand, poor core quality limited our sampling to 50 m between 500- and 700-m depth.

We also analyzed 17 samples from the 114.8- to 171.1-m depth interval in the BH-1 short core (178 m) which was drilled during the 35th Soviet Antarctic expedition in 1989-1990. These samples provided a high-resolution record covering the last 3 kyr.

Both the 3Γ and the BH-1 short cores were drilled using a thermal drill. As a result, core quality is poor at shallow depths. There are two indications that the accuracy of our results for samples above 1000 mbs may have been slightly compromised by this poor core quality. First, $\delta^{18}O_{atm}$ in the Holocene samples of Vostok is significantly greater than the modern atmospheric value adopted as the reference and therefore defined to be 0‰. The mean $\delta^{18}O_{atm}$ of samples with ages < 2.5 kyr is 0.19 ± 0.09‰ (1σ,n = 21). Analyses of samples in this age range from the high-quality GISP II core, indicate that the $\delta^{18}O$ of atmospheric O_2 has been 0.1± 0.1‰ (1σ,n = 32) during this interval (T. Sowers and M. Bender, unpublished data, 1993). Second, some adjacent samples indicate abrupt changes in $\delta^{18}O$ which are geochemically unreasonable given the 2-kyr turnover time of atmospheric O_2. Thus the uncertainty in $\delta^{18}O_{atm}$ in the upper part of the Vostok core is greater than our precision; we assign a value of ± 0.2‰. There is no reason to believe that there is any such error in samples below 1,000-m depth (~60 ka), where preservation is very good.

A plot of $\delta^{18}O_{atm}$ versus depth in the Vostok cores was constructed by connecting average $\delta^{18}O_{atm}$ values at each depth (Figure 2). The average standard deviation about the mean of all 95 depths is ±0.05‰. We compare the δD_{ice} record from Jouzel et al. [1987] with the $\delta^{18}O_{atm}$ record in Figure 2. In general, high $\delta^{18}O_{atm}$ values are associated with low δD_{ice} values which are generally thought to be indicative of colder periods.

In order to compare our $\delta^{18}O_{atm}$ data with the $\delta^{18}O_{sw}$ record in the time domain, we utilize the Lorius et al. [1985] ice chronology and the Δage estimates from Barnola et al. [1991]. Today, in the Vostok region of Antarctica, air parcels are being occluded into bubbles between 95 and 105 mbs [Barnola et al., 1987; Barnola et al., 1991]. The age of the ice at these two depths is 2,600 and 3,000

TABLE 1. Results of Trapped Gas Analysis From the Vostok Ice Core

Sample Depth, mbs	Ice Age,[a] ka	Gas Age,[b] ka	Trapped Gases $\delta^{15}N$, ‰	Trapped Gases $\delta^{18}O$, ‰	$\delta^{18}O$ of Atmospheric O_2, ‰
114.8a	3.6	0.8	0.48	1.10	0.13
114.8b			0.39	0.93	0.15
116.3a	3.7	0.9	0.46	1.12	0.20
116.3b			0.40	1.06	0.25
120.3a	3.8	1.1	0.49	1.09	0.11
120.3b			0.49	1.15	0.16
125.2a	4.0	1.3	0.43	1.07	0.20
125.2b			0.45	1.05	0.16
130.1a	4.2	1.5	0.37	1.01	0.26
130.1b			0.39	1.09	0.31
135.3a	4.4	1.7	0.50	1.11	0.10
135.3b			0.45	1.27	0.37
139.7a	4.6	1.9	0.48	1.04	0.08
139.7b			0.43	1.08	0.22
139.8a	4.6	1.9	0.39	1.11	0.33
139.8b			0.38	1.11	0.35
143.7a	4.7	2.1	0.50	1.11	0.10
143.7b			0.49	1.11	0.12
149.6a	5.0	2.3	0.43	1.02	0.15
149.6b			0.47	1.08	0.15
152.8	5.1	2.5	0.47	1.05	0.11
156.9	5.3	2.6	0.51	1.14	0.12
161.8a	5.5	2.8	0.49	1.03	0.05
161.8b			0.44	1.00	0.13
165.1a	5.6	3.0	0.49	1.05	0.07
165.1b			0.49	1.06	0.08
166.8a	5.7	3.1	0.49	1.13	0.15
166.8b			0.46	1.07	0.15
169.7a	5.8	3.2	0.48	1.04	0.07
169.7b			0.63	1.29	0.04
169.7c			0.46	0.97	0.04
174.6	5.9	3.3	0.47	1.00	0.06
177.1a	6.1	3.5	0.54	1.33	0.24
177.1b			0.45	1.14	0.24
184.3a	6.4	3.8	0.40	1.04	0.25
184.3b			0.39	1.24	0.46
213.8a	7.7	5.1	0.43	0.81	-0.05
213.8b			0.42	0.88	0.04
269.5a	10.2	7.6	0.45	0.87	-0.03
269.5b			0.41	0.95	0.13
294.5a	11.5	8.7	0.42	1.17	0.33
294.5b			0.48	1.31	0.34
303.6a	11.9	9.1	0.46	1.42	0.50
331.4a	13.5	10.2	0.43	1.74	0.89
331.4b			0.43	1.85	1.00
356.8a	15.1	11.5	0.37	1.95	1.21

TABLE 1. (continued)

Sample Depth, mbs	Ice Age,[a] ka	Gas Age,[b] ka	Trapped Gases $\delta^{15}N$, ‰	Trapped Gases $\delta^{18}O$, ‰	$\delta^{18}O$ of Atmospheric O_2, ‰
356.8b			0.39	2.11	1.33
381.5a	16.9	12.8	0.38	2.15	1.39
381.5b			0.35	2.20	1.49
409.0a	19.0	14.1	0.38	2.05	1.29
409.0b			0.38	2.10	1.35
434.2a	21.1	15.3	0.42	2.06	1.23
434.2b			0.41	2.11	1.30
443.7a	21.9	15.8	0.54	1.94	0.86
443.7b			0.39	1.92	1.15
483.7a	25.2	19.1	0.48	2.06	1.10
483.7b			0.41	1.93	1.11
534.5a	29.4	24.0	0.51	1.49	0.46
534.5b			0.47	1.54	0.60
585.5a	33.4	28.2	0.41	1.69	0.87
585.5b			0.39	1.72	0.95
656.5	39.0	33.7	0.39	1.40	0.62
694.5a	41.9	36.6	0.35	1.28	0.58
694.5b			0.29	1.24	0.66
759.8a	46.8	41.6	0.38	1.24	0.48
759.8b			0.37	1.28	0.53
788.5a	49.0	44.0	0.48	1.30	0.35
788.5b			0.50	1.38	0.39
806.2a	50.3	45.6	0.38	1.23	0.48
806.2b			0.38	1.32	0.56
834.2a	52.4	47.8	0.32	1.22	0.58
834.2b			0.35	1.32	0.63
857.6a	54.2	49.6	0.39	1.23	0.45
857.6b			0.32	1.26	0.61
885.6a	56.3	51.9	0.31	1.34	0.71
885.6b			0.31	1.33	0.71
908.2	58.1	53.7	0.35	1.58	0.87
934.4a	60.3	55.6	0.33	1.62	0.97
934.4b			0.33	1.76	1.09
937.3	60.6	55.8	0.40	1.70	0.89
957.4a	62.3	57.3	0.33	1.57	0.90
957.4b			0.34	1.61	0.93
982.3a	64.5	59.0	0.41	1.61	0.79
982.3b			0.30	1.62	1.02
1003.4a	66.3	60.7	0.38	1.67	0.92
1003.4b			0.37	1.73	1.00
1017.2a	67.5	61.9	0.38	1.71	0.96
1017.2b			0.33	1.73	1.08
1037.7a	69.2	63.8	0.33	1.37	0.72
1037.7b			0.39	1.67	0.89
1060.5a	71.2	65.9	0.35	1.59	0.88
1060.5b			0.32	1.67	1.02
1082.0a	72.9	67.9	0.36	1.39	0.68

TABLE 1. (continued)

Sample Depth, mbs	Ice Age,[a] ka	Gas Age,[b] ka	Trapped Gases $\delta^{15}N$, ‰	Trapped Gases $\delta^{18}O$, ‰	$\delta^{18}O$ of Atmospheric O_2, ‰
1082.0b			0.34	1.42	0.74
1108.4a	75.1	70.4	0.37	1.28	0.53
1108.4b			0.34	1.35	0.67
1134.6	77.2	72.7	0.33	1.26	0.60
1157.7a	79.0	74.7	0.37	1.00	0.26
1157.7b			0.31	1.10	0.48
1162.5a	79.4	75.2	0.37	0.89	0.15
1162.5b			0.33	0.95	0.30
1181.3a	80.8	76.9	0.36	0.73	0.01
1181.3b			0.32	0.79	0.15
1205.5a	82.7	79.0	0.32	0.74	0.11
1205.5b			0.28	0.96	0.41
1233.8a	84.9	81.3	0.29	0.87	0.29
1233.8b			0.33	1.03	0.37
1265.2a	87.3	83.3	0.37	1.41	0.67
1265.2b			0.31	1.37	0.75
1290.4	89.2	85.0	0.30	1.29	0.70
1307.7a	90.6	86.2	0.35	1.19	0.49
1307.7b			0.29	1.13	0.56
1309.5a	90.7	86.3	0.39	1.27	0.50
1309.5b			0.31	1.15	0.52
1333.3a	92.6	88.4	0.27	1.12	0.58
1333.3b			0.29	1.28	0.70
1363.7a	95.0	90.9	0.34	1.38	0.70
1363.7b			0.36	1.56	0.84
1391.2a	97.2	93.2	0.32	1.27	0.63
1391.2b			0.32	1.33	0.69
1419.7a	99.5	95.8	0.37	1.16	0.41
1419.7b			0.36	1.17	0.45
1443.0a	101.5	97.9	0.33	0.89	0.23
1443.0b			0.32	0.94	0.30
1467.7a	103.6	100.1	0.29	0.69	0.11
1467.7b			0.27	0.68	0.14
1494.3a	106.1	102.3	0.28	0.77	0.21
1494.3b			0.29	0.81	0.22
1505.0a	107.1	103.2	0.41	0.80	-0.03
1505.0b			0.35	0.75	0.05
1514.3	108.0	104.0	0.41	0.97	0.16
1566.2a	113.0	108.3	0.40	1.58	0.77
1566.2b			0.41	1.63	0.80
1592.0a	115.3	110.5	0.42	1.71	0.88
1592.0b			0.39	1.76	0.97
1636.3a	119.0	115.1	0.38	1.67	0.90
1636.3b			0.36	1.68	0.96
1656.1a	120.6	117.2	0.58	1.60	0.44
1656.1b			0.40	1.53	0.73
1683.3a	122.6	119.6	0.38	1.22	0.47

TABLE 1. (continued)

Sample Depth, mbs	Ice Age,[a] ka	Gas Age,[b] ka	Trapped Gases $\delta^{15}N$, ‰	Trapped Gases $\delta^{18}O$, ‰	$\delta^{18}O$ of Atmospheric O_2, ‰
1683.3b			0.38	1.26	0.50
1693.1a	123.3	120.4	0.50	1.14	0.13
1693.1b			0.50	1.14	0.14
1716.7a	125.0	122.3	0.46	0.86	-0.05
1716.7b			0.42	0.89	0.04
1732.7	126.1	123.5	0.43	0.88	0.01
1757.0a	127.8	125.2	0.43	0.78	-0.08
1757.0b			0.35	0.68	-0.03
1784.3a	129.7	127.3	0.40	0.61	-0.18
1784.3b			0.41	0.71	-0.11
1823.5a	132.5	130.3	0.41	0.76	-0.05
1823.5b			0.40	0.80	0.00
1831.9a	133.2	131.0	0.56	1.03	-0.08
1831.9b			0.51	1.06	0.05
1845.2a	134.1	132.1	0.43	1.19	0.34
1845.2b			0.40	1.20	0.41
1858.0a	135.1	133.0	0.50	1.42	0.43
1858.0b			0.44	1.39	0.51
1868.5	135.9	133.7	0.48	1.81	0.85
1882.3a	137.0	134.6	0.44	2.03	1.16
1882.3b			0.39	2.02	1.23
1883.4a	137.1	134.7	0.47	2.03	1.08
1883.4b			0.49	2.10	1.12
1907.6a	139.2	136.4	0.47	2.24	1.30
1907.6b			0.43	2.19	1.33
1907.6c			0.43	2.22	1.36
1934.5a	141.9	138.3	0.41	2.22	1.40
1934.5b			0.40	2.26	1.45
1954.6a	144.2	139.8	0.34	2.04	1.37
1954.6b			0.38	2.21	1.46
1955.8a	144.3	139.9	0.39	2.08	1.31
1955.8b			0.34	2.01	1.32
1965.5a	145.5	140.7	0.35	2.01	1.31
1965.5b			0.33	2.08	1.41
1982.3a	147.9	142.4	0.36	1.94	1.22
1982.3b			0.35	1.94	1.24
1990.8a	149.2	143.4	0.47	1.98	1.04
1990.8b			0.44	1.97	1.09
2016.4a	153.4	147.6	0.41	1.90	1.09
2016.4b			0.29	1.71	1.14
2058.8a	160.5	154.4	0.45	1.64	0.74
2058.8b			0.43	1.71	0.84

Columns 4 and 5 are the isotopic composition of trapped N_2 and O_2, respectively, relative to the present-day atmosphere. The last column is $\delta^{18}O_{atm}$, the paleoatmospheric $\delta^{18}O$ of O_2 after correction for gravitational fractionation (equation (2)). Note that mbs indicates meters below the surface.

[a] Data are from Lorius et al. [1985].

[b] Data are from Barnola et al. [1991].

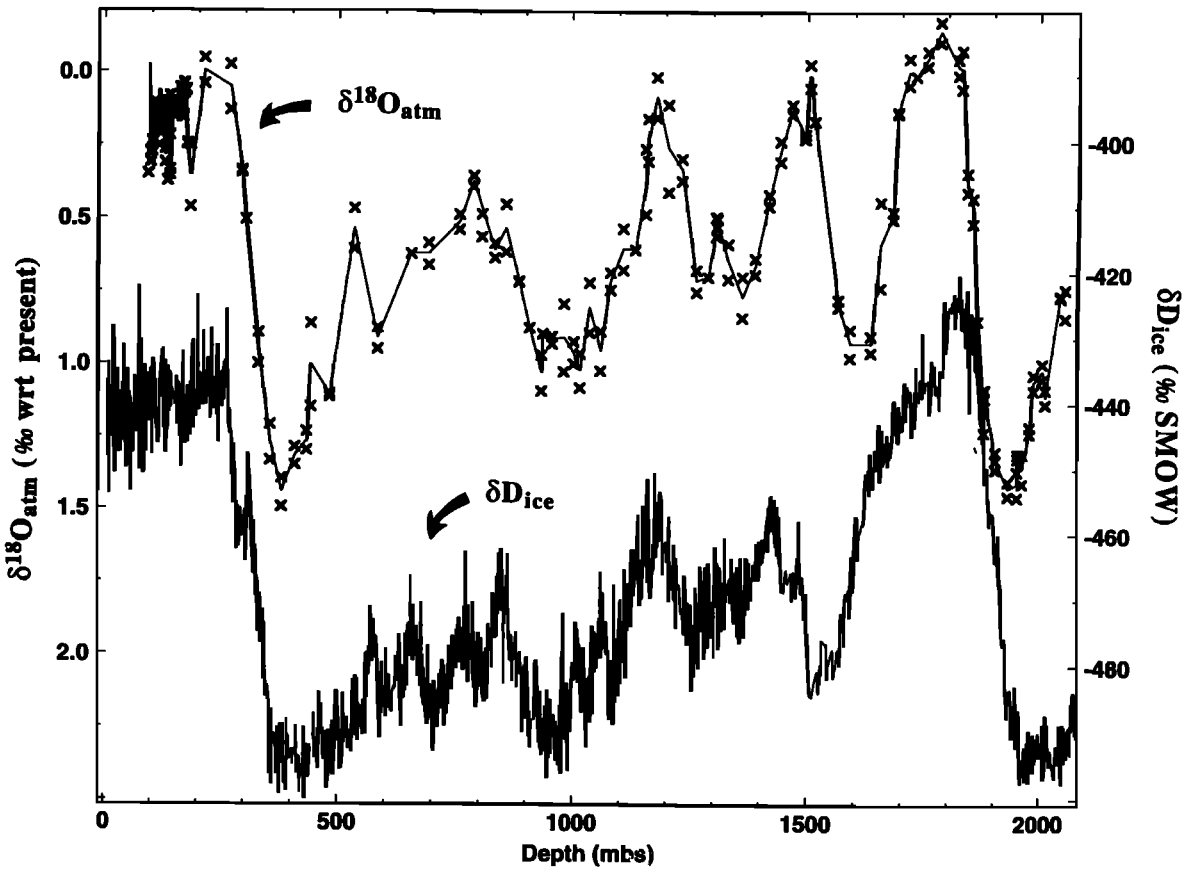

Fig. 2. Isotopic composition of paleoatmospheric O_2 ($\delta^{18}O_{atm}$) based on the isotopic composition of trapped O_2 in the Vostok ice core (top). Results are reported relative to the present-day atmosphere. The results from each analysis are plotted (with crosses) along with a line joining all the average values at each depth. Also plotted is the δD_{ice} record from Jouzel et al. [1987] (bottom). Low $\delta^{18}O_{atm}$ values are generally associated with high δD_{ice} values.

years B.P. respectively [Jouzel et al., 1987], which implies that the bubbles of air which have recently formed near Vostok are between 2,600 and 3,000 years younger than the surrounding ice. For this study, Δage is taken as the age of the firn at midpoint of the close off depth interval.

Our $\delta^{18}O_{atm}$ data are plotted in Figure 3 versus age according to the Vostok gas chronology of Barnola et al. [1991]. We also plot the $\delta^{18}O_{sw}$ record, discussed previously, versus age according to the SPECMAP chronology. The range of $\delta^{18}O$ values for the two records is similar, 1.3‰ and 1.6‰ for $\delta^{18}O_{sw}$ and $\delta^{18}O_{atm}$, respectively. The general forms of the two records are strikingly similar. The divergence between the two records for ages > 110 ka can easily be accounted for given uncertainties in the timescales.

Geochemical Controls on the $\delta^{18}O$ of Atmospheric O_2: The Morita-Dole Effect

Morita [1935], Dole [1935], Dole et al. [1954], and Kroopnick and Craig [1972] have shown that the $\delta^{18}O$ of atmospheric O_2 today is +23.5‰ relative to standard mean ocean water. This 23.5‰ difference between atmospheric O_2 and seawater is referred to as the Morita-Dole effect (hereinafter referred to as the M-D effect). The M-D effect results from oxygen isotope fractionation associated with the photosynthetic production of O_2 both on land and in the ocean, and from fractionation associated with the consumption of O_2 during aerobic respiration.

As noted by Sowers et al. [1991], there are at least four factors which may have caused $\delta^{18}O_{atm}$ in the past to be different from today's value. First, changes in $\delta^{18}O_{sw}$ result from changes in continental ice volume and directly impact the $\delta^{18}O$ of photosynthetic O_2 produced in the ocean. Changes in $\delta^{18}O_{sw}$ also affect the $\delta^{18}O$ of water evaporating from the ocean, the $\delta^{18}O$ of precipitation on the continents, and ultimately, the $\delta^{18}O$ of photosynthetic O_2 produced on the continents. Second, changes in the hydrologic cycle on glacial/interglacial timescales influence the $\delta^{18}O$ of leaf water and thereby the $\delta^{18}O$ of photosynthetic O_2

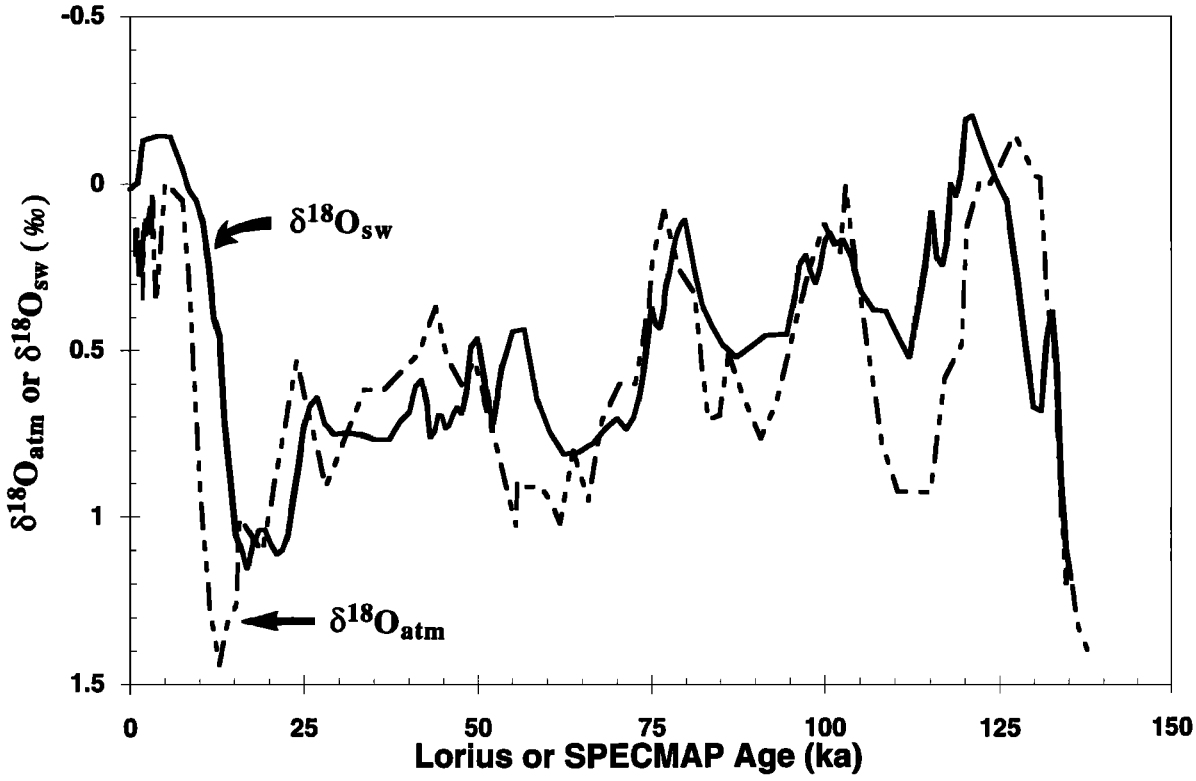

Fig. 3. Records of the $\delta^{18}O_{atm}$ (dashed line) and $\delta^{18}O_{sw}$ (solid line) from V19-30 plotted on the Barnola et al. [1991] and SPECMAP [Martinson et al., 1987] timescales, respectively. The $\delta^{18}O_{atm}$ record is reported relative to the present-day atmosphere. The $\delta^{18}O_{sw}$ record has been constructed from the $\delta^{18}O_{foram}$ record from V19-30 as noted in the text. It has been normalized by subtracting 3.46‰ from all $\delta^{18}O_{sw}$ values, so that the average $\delta^{18}O_{sw}$ during the Holocene is 0‰. Some of the discrepancies between the two records may be due to chronological inconsistencies between the two timescales. Between warm periods, the $\delta^{18}O_{atm}$ record shows much larger variations than the $\delta^{18}O_{sw}$ record, suggesting that $\delta^{18}O_{atm}$ may not be an ideal proxy for $\delta^{18}O_{sw}$, especially during these periods.

produced on the continents. Third, ecological changes over glacial/interglacial timescales cause the global average of the respiratory isotope effect to change. One can imagine such changes resulting either from changes in the make-up of the marine and continental biospheres or from changes in the isotope effects on the species level. Finally, changes in the ratio of continental to marine gross primary productivity may have had a large effect on $\delta^{18}O_{atm}$, because the $\delta^{18}O$ of leaf water is generally heavier than that of seawater. For reference, the residence time of atmospheric O_2 today, with respect to photosynthesis and respiration, is estimated to be between 2,000 and 3,000 years [Bender et al., 1985].

We can gain some insight into the factors which have influenced $\delta^{18}O_{atm}$ by examining Figure 3 in more detail. If we assume, for the moment, that some of the offset between the $\delta^{18}O_{sw}$ and $\delta^{18}O_{atm}$ is the result of chronological inconsistencies, then the high degree of covariation between the two records implies that the major factor influencing $\delta^{18}O_{atm}$ is changes in $\delta^{18}O_{sw}$. As we mentioned previously, the range of $\delta^{18}O_{atm}$ values is similar to the $\delta^{18}O_{sw}$ values over the last 150 kyr. This result suggests that the biologic and hydrologic factors which influence $\delta^{18}O_{atm}$ have remained close to their present-day values. For example, a 30% change in the ratio of marine to terrestrial productivity would produce a change of about 0.5‰ in $\delta^{18}O_{atm}$ relative to $\delta^{18}O_{sw}$. The only time when a change of this magnitude is suggested by the data is during marine isotope stage 5d (110 ka). We cannot rule out the possibility that there were substantial changes in the biologic and hydrologic cycles which had no net effect on $\delta^{18}O_{atm}$, but we consider it unlikely given the similar nature of the two curves in Figure 3.

From the similarity of the two curves in Figure 3

we tentatively conclude that (1) the major factor influencing $\delta^{18}O_{atm}$ appears to be $\delta^{18}O_{sw}$, (2) there are periods when the M-D effect was substantially different than it is today, and (3) the degree to which the first two conclusions may be considered valid depends on how well we can correlate the Vostok and SPECMAP chronologies.

We will now turn our attention to the development of the gas age versus depth relation for Vostok. As mentioned previously, we derive this relation by correlating our measured $\delta^{18}O_{atm}$ record with the $\delta^{18}O_{sw}$ record from V19-30 (Figure 3) using the inverse correlation method developed by Martinson et al. [1982]. We then test the fidelity of this common framework by comparing temperature records from the two media.

CONSTRUCTION OF A "COMMON TEMPORAL FRAMEWORK"

Establishing a Gas Age-Depth Curve for Vostok

Based on the good agreement between the $\delta^{18}O_{atm}$- age and $\delta^{18}O_{sw}$- age records, we conclude that the major factor causing changes in $\delta^{18}O_{atm}$ is variability in $\delta^{18}O_{sw}$. We now assume that the M-D effect has been constant at the modern value of +23.5‰ during the period of our study and derive a curve of gas age versus depth for the Vostok ice core by correlating the Vostok curve of $\delta^{18}O_{atm}$ versus depth into the V19-30 curve of $\delta^{18}O_{sw}$ versus age [Martinson et al., 1982; Martinson et al., 1987]. Before proceeding, we note that there were times when the M-D effect clearly deviated from the modern value. Thus the correlation that we derive is based on an assumption which is not completely correct and will undoubtedly need to be further refined.

The first step in deriving our age-depth curve for Vostok was to choose the deepest and shallowest depths we wished to correlate and assign ages to these two depths. As an upper bound, we choose our shallowest sample from 114.8 mbs. The ice age at 114.8 mbs is 3.6 ka [Lorius et al., 1985]; the age of the trapped air parcels at 114.8 mbs, calculated using the Δage values of Barnola et al. [1991] (2.8 kyr), is then 0.8 ka (3.6 ka - 2.8 kyr). Because the turnover time of atmospheric O_2 is about 2 kyr, the $\delta^{18}O_{atm}$ of trapped gas dated to be 0.8 ka reflects the $\delta^{18}O$ of seawater at 2.8 ka [Sowers et al., 1991].

We choose the depth of 1934.5 mbs as the bottom of our correlation interval. The $\delta^{18}O_{atm}$ reaches a maximum at this depth which corresponds to the $\delta^{18}O_{sw}$ maximum, dated at 135 ka in the SPECMAP chronology. This period corresponds to the glacial maximum preceding the penultimate deglaciation.

After tying the end-points of the two records, we applied a 1.0-cycle/kyr filter to the $\delta^{18}O_{atm}$ record and correlated the two records using the protocol developed by Martinson et al. [1982]. The correlation involves the construction of a mapping function (in our case a correlated gas age-depth curve) for the Vostok ice core. The mapping function consists of a sum of sinusoids (of increasing order) which have amplitudes chosen to maximize the amount of shared variance between the two $\delta^{18}O$ records. The number of sinusoids added to the mapping function determines the resolution of the correlation. In our case, we stopped the correlation at a resolution of ~17 kyr (8 sinusoids). We chose to correlate the two records at this modest level of resolution because the characteristic response time for an ice sheet which has been subjected to changes in accumulation rate is approximately 17 kyr [Imbrie et al., 1984]. The correlation coefficient between the correlated records was 0.88 (77% shared variance between the correlated records).

By correlating the $\delta^{18}O_{atm}$ versus depth curve from Vostok into the $\delta^{18}O_{sw}$ versus age record, we infer a gas age-depth relationship for the Vostok ice core. The implied age of the trapped gas sample, which we define as the correlation age, is equal to the gas age plus the atmospheric O_2 turnover time, 2 kyr. Global productivity and hence the atmospheric O_2 turnover time undoubtedly varied during glacial-interglacial cycles. Estimates vary widely but are generally within 25% of present-day values [Lyle, 1988; Meyer, 1988; Mix, 1989]. Changes of this magnitude would introduce an error of ± 0.5 kyr to our gas ages. In Figure 4, we plot $\delta^{18}O_{atm}$ versus the Vostok correlation age and $\delta^{18}O_{sw}$ versus the SPECMAP age. This figure shows that one can derive a correlation age-depth curve for Vostok in which $\delta^{18}O_{atm}$ and $\delta^{18}O_{sw}$ track each other very well.

Figure 4 also shows that $\delta^{18}O_{atm}$ does not follow $\delta^{18}O_{sw}$ exactly and that the M-D effect must have varied during the last 135 kyr. A detailed discussion of the variable M-D effect will be presented in a forthcoming paper. The range of variability in the M-D effect (0.9‰) is about 75% as large as the range of $\delta^{18}O_{sw}$ (1.3‰), and it may clearly impart significant errors to our Vostok age-depth curve, which is derived simply by assuming that the M-D effect has been constant. It is for this reason that we consider $\delta^{18}O$ to be an equivocal correlation tool [Sowers et al., 1991].

Establishing an Ice Age-Depth Curve for Vostok

In the previous section we derived a gas age-depth relation by correlating the $\delta^{18}O_{atm}$ record from Vostok into the SPECMAP $\delta^{18}O_{sw}$ record. In order to compare the isotopic and chemical composition of the paleoprecipitation at Vostok with the marine climate records, we need to calculate an ice age-depth curve for this core. Put another way, we need to

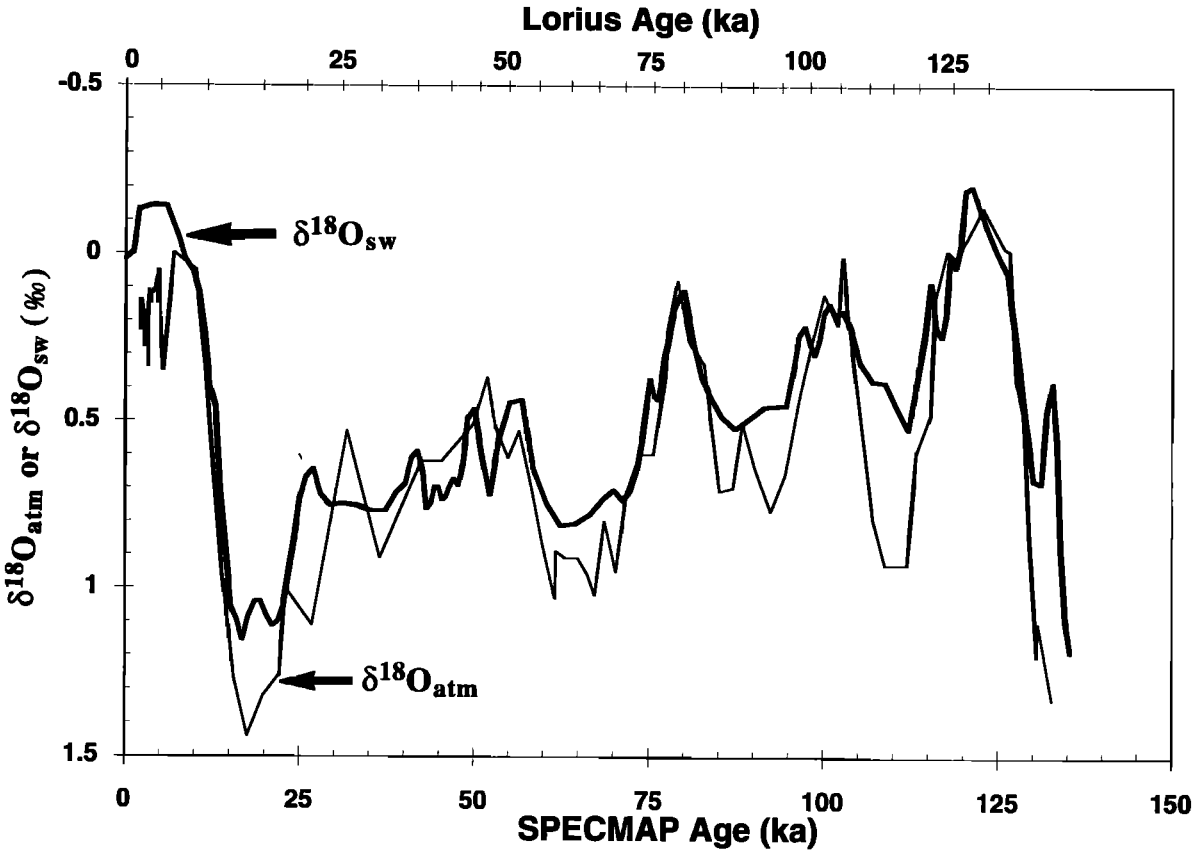

Fig. 4. Records of the $\delta^{18}O_{atm}$ (thin line) and $\delta^{18}O_{sw}$ (thick line) plotted on the SPECMAP [Martinson et al., 1987] timescale. The $\delta^{18}O_{atm}$ record has been correlated into the SPECMAP chronology using the inverse correlation method of Martinson et al. [1982]. We have purposely not tried to correlate the detailed features which are shorter than about 5 kyr. We believe the larger $\delta^{18}O_{atm}$ variations are the result of changes in ^{18}O fractionation which are most likely associated with the terrestrial biosphere. The Lorius et al. [1985] timescale is plotted on the upper axis for comparison. The $\delta^{18}O_{sw}$ record is identical to that plotted in Figure 3.

account for the fact that the air parcels were trapped at least 100 m below the surface of the ice sheet and are thus younger than the surrounding ice. We refer to this age difference as the ice age-gas age difference (Δage). We have utilized a densification model [Herron and Langway, 1980], the record of the paleoaccumulation rate from our correlated gas age-depth curve, and an estimate of the thinning function [Ritz, 1992] to calculate a record of the paleo-close-off depth and Δage all along the core. Results of these calculations suggest that paleo-close-off depths varied between 100 and 125 m below the surface with corresponding Δage values ranging from 2.9 to 7.0 kyr, respectively [Sowers et al., 1992]. Deeper close-off depths and larger values of Δage occur during glacial periods when the temperature and accumulation rate were low. The appendix contains a detailed explanation of these factors and the associated errors. The resulting ice ages for each of our sample depths are listed in Table 2.

IMPLICATIONS FOR CLIMATE LEADS AND LAGS

Sowers et al. [1991] compared the depths at which the $\delta^{18}O$ of O_2 and pCO_2 began to change at the beginning of the penultimate termination. They found that $\delta^{18}O$ of O_2 began to fall approximately 6 kyr before pCO_2 began to rise. They concluded that the pCO_2 rise led the $\delta^{18}O_{sw}$ decrease by 4 ± 1.7 kyr (the response time of the $\delta^{18}O$ of atmospheric O_2 to a change in $\delta^{18}O$ of seawater is about 2 kyr). The age-depth curve of Pichon et al. [1992] supports this conclusion, as it puts the start of the pCO_2 rise (and

TABLE 2. Vostok Ice Core Correlation Ages

Sample Depth, mbs	Gas Age, ka	Ice Age, ka		Correlated Ice Age - Lorius Ice Age, ka
		Correlated	Lorius[a]	
114.8	0.8	3.9	3.6	0.3
116.3	0.9	4.0	3.6	0.4
120.3	1.1	4.1	3.8	0.3
125.2	1.3	4.3	4.0	0.3
130.1	1.5	4.5	4.2	0.3
135.3	1.7	4.8	4.4	0.4
139.7	1.9	4.9	4.6	0.3
139.8	1.9	4.9	4.6	0.3
143.7	2.0	5.1	4.7	0.4
149.6	2.3	5.3	5.0	0.3
152.8	2.4	5.5	5.1	0.4
156.9	2.6	5.6	5.3	0.3
161.8	2.8	5.8	5.5	0.3
165.1	2.9	6.0	5.6	0.4
166.8	3.0	6.0	5.7	0.3
169.7	3.1	6.1	5.8	0.3
174.6	3.3	6.4	5.9	0.5
177.1	3.4	6.5	6.1	0.4
184.3	3.7	6.8	6.4	0.4
213.8	5.0	8.1	7.7	0.4
269.5	8.0	11.7	10.2	1.5
294.5	9.5	14.0	11.5	2.5
303.6	10.1	14.8	11.9	2.9
331.4	11.9	17.4	13.5	3.9
356.8	13.7	20.4	15.1	5.3
381.5	15.6	23.9	16.9	7.0
409.0	17.9	25.8	19.0	6.8
434.2	20.2	27.8	21.1	6.7
443.7	21.0	28.7	21.9	6.8
483.7	24.9	32.0	25.2	6.8
534.5	29.8	36.3	29.4	6.9
585.5	34.5	40.2	33.4	6.8
656.5	40.4	45.7	39.0	6.7
694.5	43.3	48.3	41.9	6.4
759.8	47.9	52.5	46.8	5.7
788.5	49.9	54.3	49.0	5.3
806.2	51.1	55.8	50.3	5.5
834.2	52.9	57.3	52.4	4.9
857.6	54.5	58.5	54.2	4.3
885.6	56.4	60.9	56.3	4.6
908.2	57.9	63.2	58.1	5.1
934.4	59.6	65.4	60.3	5.1
937.3	59.8	65.6	60.6	5.0
957.4	61.2	66.8	62.3	4.5
982.3	62.9	67.9	64.5	3.4
1003.4	64.4	68.5	66.3	2.2
1017.2	65.3	69.4	67.5	1.9
1037.7	66.8	71.2	69.2	2.0
1060.5	68.4	72.7	71.2	1.5
1082.0	69.9	74.3	72.9	1.4
1108.4	71.8	76.1	75.1	1.0
1134.6	73.6	77.4	77.2	0.2

TABLE 2. (continued)

Sample Depth, mbs	Gas Age, ka	Ice Age, ka		Correlated Ice Age - Lorius Ice Age, ka
		Correlated	Lorius[a]	
1157.7	75.3	78.7	79.0	-0.3
1162.5	75.7	79.1	79.4	-0.3
1181.3	77.0	80.8	80.8	0.0
1205.5	78.8	82.7	82.7	0.0
1233.8	80.9	85.3	84.9	0.4
1265.2	83.2	87.9	87.3	0.6
1290.4	85.1	89.5	89.2	0.3
1307.7	86.4	90.1	90.6	-0.5
1309.5	86.5	90.2	90.7	-0.5
1333.3	88.3	92.4	92.6	-0.2
1363.7	90.5	94.7	95.0	-0.3
1391.2	92.5	96.5	97.2	-0.7
1419.7	94.6	98.3	99.5	-1.2
1443.0	96.3	100.0	101.5	-1.5
1467.7	98.1	102.2	103.6	-1.4
1494.3	100.0	104.3	106.1	-1.8
1505.0	100.8	105.3	107.1	-1.8
1514.3	101.5	106.3	108.0	-1.7
1566.2	105.1	109.3	113.0	-3.7
1592.0	106.9	110.4	115.3	-4.9
1636.3	110.0	112.8	119.0	-6.2
1656.1	111.3	114.1	120.6	-6.5
1683.3	113.2	116.1	122.6	-6.5
1693.1	113.9	116.8	123.3	-6.5
1716.7	115.6	118.5	125.0	-6.5
1732.7	116.8	119.7	126.1	-6.4
1757.0	118.6	121.5	127.8	-6.3
1784.3	120.7	123.6	129.7	-6.1
1823.5	123.7	126.4	132.5	-6.1
1831.9	124.4	127.0	133.2	-6.2
1845.2	125.5	128.2	134.1	-5.9
1858.0	126.6	129.5	135.1	-5.6
1868.5	127.4	130.4	135.9	-5.5
1882.3	128.6	131.9	137	-5.1
1883.4	128.7	132.0	137.1	-5.1
1907.6	130.7	134.7	139.2	-4.5
1934.5	133.0	136.8	141.9	-5.1

Gas ages are those derived from the inverse correlation of the $\delta^{18}O_{atm}$ record with the $\delta^{18}O_{sw}$ record from V19-30 core. The third column lists the ice ages from the correlation (see text for details). The last column lists the difference between the correlated ice ages and those from the Lorius et al. [1985]. Note that mbs indicates meters below the surface.

[a] Data are from Lorius et al. [1985].

warming at Vostok) at about 139 ka in the SPECMAP chronology, while the $\delta^{18}O$ of seawater begins to decrease at about 135 ka in this chronology. Both the radiolarian chronology [Shackleton et al., 1992] and the diatom chronology [Pichon et al., 1992] indicate a lag at the end of the termination: CO_2 reached its maximum value at about 129 ka in these chronologies (and about 126 ka in our chronology), while the $\delta^{18}O_{sw}$ minimum was about 123-125 ka according to the SPECMAP chronology. The work summarized here thus indicates that CO_2 changes led the ice volume decrease throughout the penultimate termination.

COMPARISON OF AGE-DEPTH CURVES PROPOSED FOR THE VOSTOK ICE CORE

Our age-depth curve, like others recently proposed for the Vostok ice core [Petit et al., 1990; Pichon et al., 1992; Shackleton et al., 1992], generally agrees very well with the "flow model" chronology proposed by Lorius et al. [1985]. The correlated ice age-depth curve deviates from the Lorius et al. [1985] curve by more than 2 kyr between 350 and 1000 mbs and again below 1500 mbs (Figure 5). Our correlation of Vostok into the SPECMAP chronology requires increasing the Lorius et al. [1985] age for the beginning of termination I by 5 kyr and decreasing the age for the start of termination II by 5 kyr. Our chronology is in excellent agreement with the Lorius et al. [1985] chronology for the interval between 70 and 110 ka (roughly 1050 to 1580 mbs).

Our age-depth curve is compared with similar curves recently proposed by other workers (Figure 5). Petit et al. [1990] picked control points by aligning the "magnetic flux" record from the marine sediment core RC11-120 with dust accumulation near Vostok (we refer to this correlation technique as the dust correlation). Pichon et al. [1992] picked control points by aligning the temperature - depth record for Vostok with the record of SST versus age

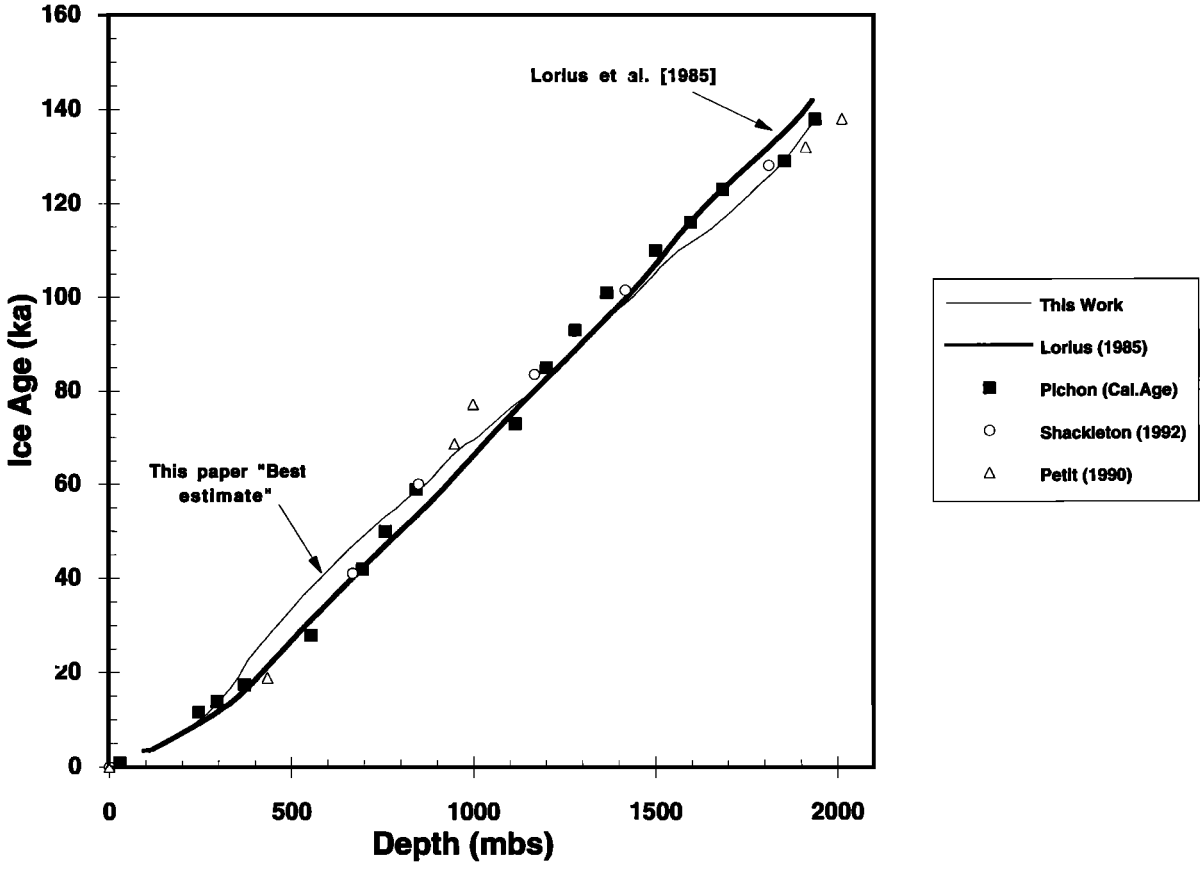

Fig. 5. Various ice age versus depth profiles for the Vostok ice core. The curve labeled "Best estimate" is based on our $\delta^{18}O$ correlation. Also plotted are the estimate by Lorius et al. [1985] and the "control points" of Pichon et al. [1992] (diatom), Shackleton et al. [1992] (radiolaria), and Petit et al. [1990] (dust). In general, all recent correlations agree with the original model of Lorius et al. [1985] within stated uncertainties.

for southern ocean core MD 84-551. SST for this core was inferred from diatom taxonomy using a transfer function (the diatom correlation). Shackleton et al. [1992] picked control points by aligning the temperature-depth record for Vostok with the SST record of core RC11-120, determined from radiolarian taxonomy (the radiolarian correlation) [Hays et al., 1976*a,b*]. For this latter record we have plotted only control points associated with maximum SST values; SST minima might not be faithfully reflected given the limited temperature range of radiolarian species.

Between about 290- and 360-m depth, the interval covering the last deglaciation, our proposed age-depth curve diverges strongly from that of Lorius et al. [1985]. We assign the 357-m depth an age of 20 kyr, compared to the flow model age of 15 kyr. As noted above, the Petit et al. [1990] chronology (dust) is in fair agreement with the flow chronology over this interval. The diatom timescale in this depth interval is based on ^{14}C dates rather than the short SPECMAP chronology (which is independent of the ^{14}C chronology). To allow a more direct comparison, we note that Martinson et al. [1987] assigned an age of 17.9 kyr for the last glacial maximum (event 2.2 in Table 2). This age is in good agreement with a sidereal age of about 18 kyr for the $\delta^{18}O_{foram}$ maximum, based on ^{14}C dating of many foraminiferal $\delta^{18}O$ curves [Sarnthein et al., 1992] after converting ^{14}C ages to absolute ages based on the work of Bard et al. [1990*a*]. When we convert the MD84-551 timescale from ^{14}C ages to absolute ages, the start of the last termination moves from 15 ka (^{14}C) to 17 ka (calendar). If we were to recorrelate the MD84-551 SST and Vostok temperature records on the calendar timescale, the Vostok temperature-age record would be in better agreement with the temperature-age record from the Byrd ice core, where the beginning of the termination is dated between 16 and 18 ka [Beer et al., 1992].

Between about 400- and 800-m depth, corresponding to correlated SPECMAP ages of 25-55 ka, our proposed correlation ages are highly uncertain. Comparing $\delta^{18}O_{atm}$ and $\delta^{18}O_{sw}$ values over this interval is problematic for two reasons. First, $\delta^{18}O_{sw}$ variations are small (total range of 0.35‰), so that there is not a strong signal. Second, sample resolution is poor because of substandard ice quality in this interval; between 500- and 650-m depth we have analyzed only 2 samples. This poor basis for correlation translates into two anomalous results in the correlated chronology. The $\delta^{18}O_{atm}$ minimum at 533-m depth, derived from a single sample, is not correlated into the $\delta^{18}O_{sw}$ minimum at 32 ka but precedes it by about 5 kyr (Figure 4). Additionally, the CH_4 concentration maximum at 625-m depth in the Vostok core, dated at 32 ka in the Lorius et al. [1985] chronology, is redated to 37 ka by our correlation with the SPECMAP chronology. This age is 6 kyr older than the maximum in low-latitude simulated precipitation calculated by Prell and Kutzbach [1987] to coincide with the maximum in northern hemisphere summer insolation at 31 ka. There is a strong precession signal in the CH_4 concentration variations [Chappellaz et al., 1990]. Chappellaz et al. [1990] explained the relationship between CH_4 maxima and maxima in simulated precipitation by suggesting that higher precipitation leads to higher rates of CH_4 production. All other CH_4 concentration maxima in the Vostok record are closely aligned with northern hemisphere summer insolation maxima given our correlated ages [M. Bender et al., The Dole effect and its variations during the last 130,000 years as measured in the Vostok ice core, submitted to Global Biogeochemical Cycles, 1993). The fact that the CH_4 maximum at 625-m depth precedes the insolation maximum by 6 kyr is another cause for concern about errors in our correlated chronology between 25 and 55 ka. Our correlated ages are less reliable for this section than for any other part to the Vostok core.

In the depth interval from 800 m to 1200 m (55-80 ka), ages inferred from $\delta^{18}O$ of O_2, diatoms, radiolaria, and dust scatter considerably but are all on average about 5 kyr older than ages at the same depth estimated from the flow model (Figure 6). In this depth interval, none of the correlation methods would be expected to work well, because variations in paleotemperature, $\delta^{18}O$ of O_2 and seawater, and dust flux are all small and therefore do not provide a strong basis for intercomparing records. In general, it can be said that the various correlation approaches give about the same accumulation rates between 800 and 1200 m as the flow model but give older absolute ages.

Between 1200 and 1600 m, ages from the flow model and $\delta^{18}O$ stratigraphy are in good agreement, and ages from dust, diatoms, and radiolaria are higher by about 4 kyr. Perhaps the most accurately dated depth in this interval is at about 1200 m, where the radiolarian record shows a distinct temperature maxima and $\delta^{18}O$ of O_2 shows clear minima corresponding to stage 5a. At this depth, dates from the flow model, from $\delta^{18}O$ of O_2 , and from radiolaria agree to within 3 kyr. Diatom ages are higher than $\delta^{18}O$ ages by about 3 kyr, and this may reflect the fact that the diatom temperature record shows more variability than, and is not easily correlated with, the ice core record in this time interval.

By 1700 m, corresponding approximately to the beginning of stage 5d, the various age-depth curves show increased divergence. Diatom ages agree well with the flow chronology, while $\delta^{18}O$ ages are about 7 kyr younger. We believe that the $\delta^{18}O$ ages are less reliable, because the $\delta^{18}O_{atm}$ is clearly not following changes in $\delta^{18}O_{sw}$ such that much of the variability in $\delta^{18}O_{atm}$ must be due to changes in the M-D effect. The radiolarian chronology of Shackleton et al. [1992] brings the time of the

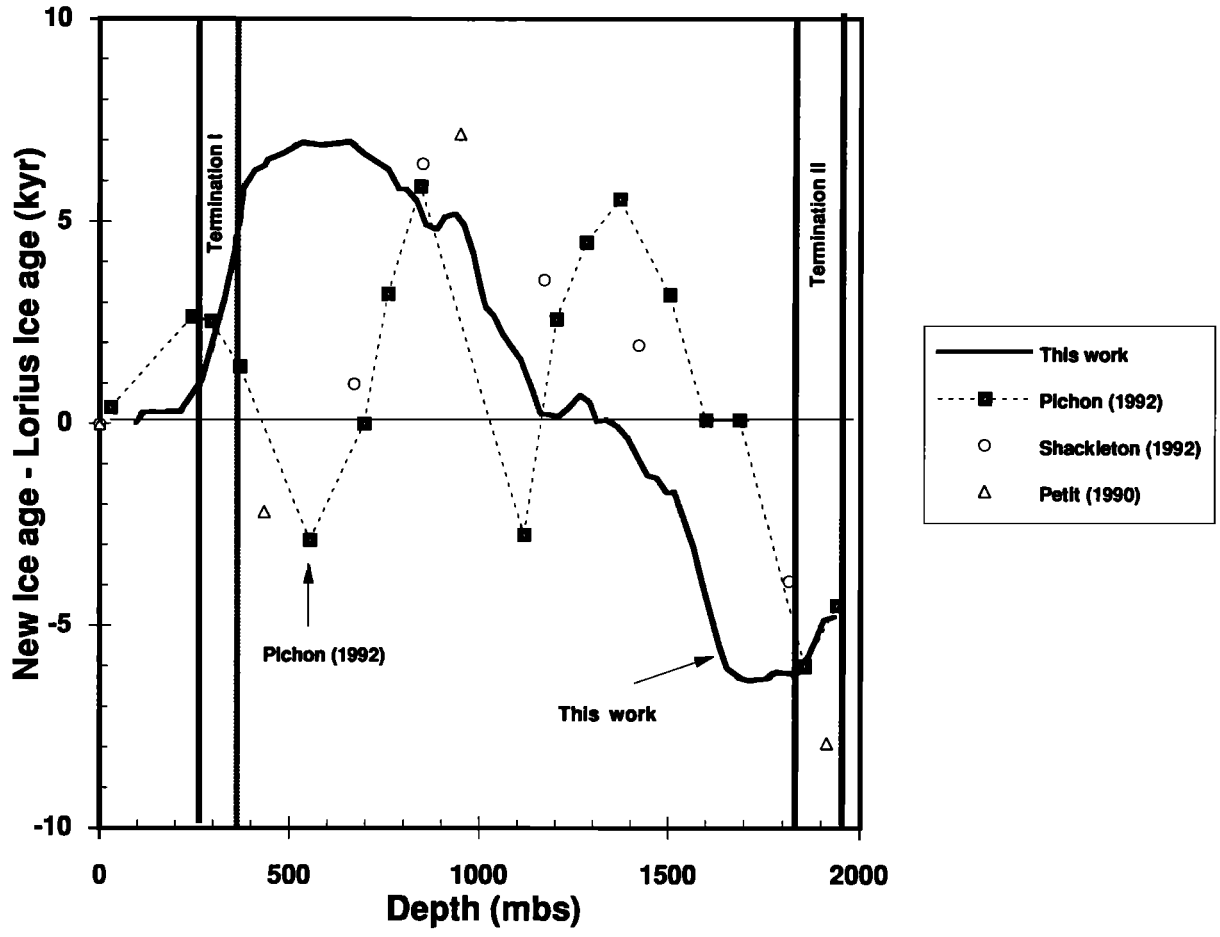

Fig. 6. Differences between the original Lorius et al. [1985] age estimates and those from recent correlation studies. The thick line illustrates the results from the $\delta^{18}O$ (ice) correlation. The dashed line illustrates the paleoaccumulation rate predicted from the Pichon et al. [1992] (diatom) correlation. Also plotted are the "control points" from Shackleton et al. [1992] (circles) and Petit et al. [1990] (triangles). Terminations I and II are marked for reference. During termination I, both the diatom and $\delta^{18}O$ correlations indicate that the ice ages are older than corresponding ages from the Lorius et al. [1985] timescale. For termination II, all correlated ages are all about 7 kyr younger than the Lorius et al. [1985] timescale. During the last glacial period, the correlated ages vary by less than ±6 kyr from the original Lorius et al. [1985] chronology.

decrease in pCO_2 observed at Vostok into line with the time of the $\Delta\delta^{13}C$ (planktonic-benthic) increase observed in both their stacked record as well as their V19-30 record. This last result must be viewed with caution, as the Δage estimates used by Shackleton et al. [1992] were not consistent with their modified ice age-depth curve.

At 1850-m depth (stage 5e), radiolarians, diatoms, and $\delta^{18}O$ all give concordant ages which are younger than that of the flow model chronology. Radiolarians and diatoms give ages of about 128 ka for the temperature minimum at stage 5e, in good agreement with the $\delta^{18}O$ age of about 126 ka. The age estimated from the flow model is about 133 ka. The dust age at a slightly deeper control point is even younger than the $\delta^{18}O$ age. Pichon et al. [1992] and Shackleton et al. [1992] have shown that Vostok temperature and pCO_2 values can be brought into phase with southern ocean SST and foram $\Delta\delta^{13}C$ values by invoking an age for the temperature

minimum which is about 5-10 kyr younger than that of the flow chronology. Our work supports their conclusions.

COMPARISON OF OTHER DEEP-SEA AND VOSTOK CLIMATE RECORDS

Southern Ocean Sea Surface Temperature Records Correlated to the Vostok Inversion Layer Temperature

We now compare temperature records from Antarctica and the southern ocean to investigate the validity of our underlying premise which is that $\delta^{18}O_{atm}$ may be used as a proxy for $\delta^{18}O_{sw}$. Because the temperature above the Antarctic inversion layer is controlled by the transport of latent and sensible heat from the southern ocean, the record of Antarctic inversion layer temperature is believed to have been similar to the SST record for the southern ocean over the same period [Pichon et al., 1992]. The δD of the precipitation over Antarctica has been shown to be controlled by the temperature at the top of the inversion layer [Jouzel and Merlivat, 1984]. The record of δD variations along the Vostok ice core have been used to construct a record of the inversion layer temperature over the Vostok area [Jouzel et al., 1987].

We assume that there is a strong relationship between southern ocean sea surface temperature and the temperature above the inversion layer. We then test the age-depth curve we derived for Vostok by comparing the Vostok curve of inversion layer temperature versus age against the southern ocean sea surface temperature-age curve (inferred from the temperature dependence of planktonic microfossils). The degree of concordance is a measure of the fidelity of our age-depth curve and the validity of the assumption that temperature is faithfully recorded by the different proxy data (diatom and radiolarian SST and δD_{ice}).

Sea surface temperature records from RC11-120 (44°31'S, 79°52'E) [Hays et al., 1976*a,b*; Lozano and Hays, 1976] and MD88-770 (46°S, 96°E) (L. Labeyrie et al., Changes in southern ocean hydrology over the last 230 kyr as recorded in core MD88-770, manuscript in preparation, 1993) are plotted in Figure 7. Relevant data from MD88-770 are also tabulated in Table 3. The temperature records are estimated from data relating the distribution of microfossils recovered from sediment core tops to the overlying sea surface temperature. The diatom record is believed to represent summer SST to about ±1°C [Pichon et al., 1992]. For both records, we estimated ages by correlating $\delta^{18}O_{foram}$-depth curves into the SPECMAP stacked $\delta^{18}O_{foram}$-age curve [Pisias et al., 1984; Martinson et al., 1987]. We then use the age versus depth relation from the $\delta^{18}O$ correlation to transfer the SST record from the depth domain to the time domain. Glacial/interglacial sea surface temperature changes inferred from the RC11-120 and MD88-770 records are about 6°-8°C.

Sea surface temperature estimates for RC11-120 are systematically higher, by about 4°C, than temperatures estimated for MD88-770. One reason is that despite their similar latitude, MD88-770 is actually located about 3° closer to the Polar Front than RC11-120. Another reason is that the radiolarian transfer function reflects temperatures below 7°C very poorly, while the diatom transfer function loses discrimination above about 10°C. We suspect that the RC11-120 record may be overestimating glacial temperatures and adopt the SST record from MD88-770 for comparison with Vostok. Both RC11-120 and MD88-770 are presently located in the subantarctic water mass which is bounded to the south by the Antarctic Polar Front and to the north by the Subtropical Convergence. Summer water temperatures between 10°C and 14°C along with salinities of 34.3-34.9‰ normally characterize the northern boundary of subantarctic water which is presently located at about 40°S. The Antarctic Polar Front has water temperatures of between 4 and 10°C with salinities between 34.0 to 34.6‰. The location of the Antarctic Polar Front is presently located just south of 50°S latitude [Lozano and Hays, 1976].

Interpreting sea surface temperature records from this region of the southern ocean is problematic, because some variability may be related to localized changes in the hydrographic setting, rather than large-scale changes in SST. In particular, migration of the Polar Front across our site, rather than regional changes in SST, may be responsible for much of the variability we observe. Two studies in particular have looked at the movement of the Polar Front in this region of the southern ocean; Hays et al. [1976*b*] studied the distribution of radiolaria, while Howard and Prell [1992] looked at the foraminiferal assemblages to determine the position of the Polar Front during the last glacial maximum period relative to the present day location. Both studies concluded that the Antarctic Polar Front was located about 4°-7° north of its present-day position during the last glacial period. Given that MD88-770 is located about 6° north of the present day Antarctic Polar Front, it is conceivable that some of the SST variability observed in Figure 7 is related to the passage of the front over the site. Nevertheless, we believe that the influence of the Polar Front has not compromised this SST record substantially for three reasons: (1) The Subantarctic assemblage has dominated the diatom population throughout the 150-ka record, as exhibited by its high-factor loadings (>62%), (2) the amount of ice-rafted debris does not increase during glacial periods, and (3) the abundance of the four diatom species which are

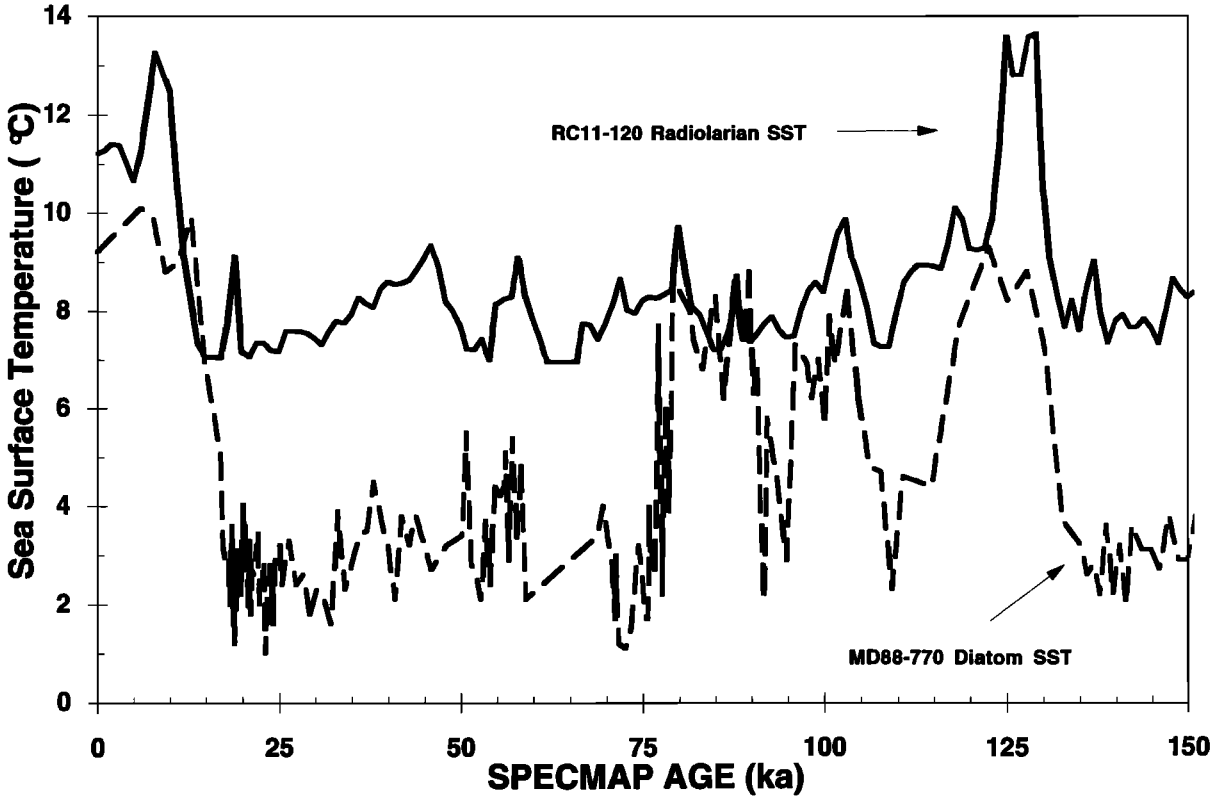

Fig. 7. Sea surface temperature (SST) records from RC11-120 (44°S, 80°E) (solid line) and MD88-770 (46°S, 96°E) (dashed line) both plotted on the SPECMAP timescale. The RC11-120 record is from Hays et al. [1976*a*] based on a radiolarian transfer function. The SST record from MD88-770 is based on a diatom transfer function [Pichon et al., 1992]. The two records show similar glacial to interglacial temperature shifts of 6°-8°C. The SST record from RC11-120 is systematically higher than that of MD88-770. One explanation for this systematic difference is that the radiolarian transfer function is not reliable at temperatures below 7°C.

associated with sea ice (*Nitzschia curta*, *Actinocyclus actinochilus*, *Nitzchia sublineata*, and *Nitzchia cylindrus*) remains low. Based on this evidence we believe that the SST record from MD88-770 can be used as a reasonable approximation of the SST record of the subantarctic waters north of the Polar Front.

Ice Core Records of Atmospheric Temperatures

Over the Antarctic continent, there is a 300- to 700 m layer of air in which the temperature increases with increasing altitude. Above this temperature inversion, temperatures decrease according to the adiabatic lapse rate. The strength of the inversion layer, as measured by the difference between the surface temperature and the temperature just above the inversion layer, is about 5°C near the coast [Phillpot and Zillman, 1970]. Maximum temperature differences reach 20°C near Vostok. As noted above, the accumulation rate and the isotopic composition of the precipitation are related to the temperature just above the inversion layer where the precipitation is formed [Robin, 1977; Jouzel and Merlivat, 1984]. We adopt the inversion layer temperature record from Jouzel et al. [1987] which is based on the measured δD profile from the Vostok core for comparison with the SST from MD88-770. In Figure 8 we have plotted the Vostok temperature record using our correlated ice age-depth relation. The SST record is plotted using the SPECMAP timescale as in Figure 7. These two records show glacial/interglacial temperature changes of 6°-8°C. Plotted in this fashion, the two records have a correlation coefficient of 0.72, implying that 52% of the variance is shared by the two records. When these two data sets are compared using the Lorius et al. [1985] chronology, the correlation coefficient is 0.54 (i.e., only ~30% shared variance). We interpret the higher degree of correlation between the two records using our common temporal framework as evidence that the Vostok record is better correlated with the deep-sea record using the chronology derived here from $\delta^{18}O_{atm}$ data. We make no claim for having improved the absolute chronology.

TABLE 3. Data From Deep-Sea Sediment Core MD88-770

Sample Depth, cm	Age, ka	Benthic $\delta^{18}O$, ‰ PDB	Sea Surface Temperature, °C
0	0.0	3.55	9.2
10	6.0	3.50	10.1
20	7.7	3.55	9.9
30	9.4	3.83	8.8
40	11.1	3.87	9.0
50	13.0	4.49	9.9
60	15.0	4.72	6.9
70	17.0	5.16	5.1
80	17.3	5.01	3.2
90	17.7	5.10	2.9
100	18.0	4.92	3.0
110	18.3	5.02	2.0
120	18.6	5.14	3.6
130	18.9	5.03	1.2
136	19.1	5.19	-
140	19.3	4.90	3.1
150	19.6	5.10	2.7
154	19.7	-	2.2
156	19.8	-	2.4
158	19.9	-	3.3
160	19.9	5.13	3.2
162	20.0	-	3.1
164	20.0	-	3.0
166	20.1	-	4.1
170	20.2	5.09	2.7
174	20.4	-	3.6
176	20.4	5.18	-
178	20.5	-	3.2
180	20.6	5.12	2.9
184	20.7	-	2.3
186	20.8	5.10	-
190	20.9	5.16	1.9
194	21.0	-	3.3
196	21.1	5.02	-
200	21.2	-	1.8
204	21.3	-	2.7
210	21.5	5.15	2.6
214	21.7	-	2.7
220	21.9	5.06	3.2
224	22.0	5.04	2.9
226	22.1	5.05	2.8
230	22.2	-	3.5
234	22.3	-	2.0
236	22.4	5.04	-
240	22.5	5.06	2.1
244	22.6	-	2.4
246	22.7	4.98	-
250	22.8	-	2.4
254	23.0	-	2.8
260	23.2	-	1.0
264	23.3	-	1.4
270	23.5	-	2.2

TABLE 3. (continued)

Sample Depth, cm	Age, ka	Benthic $\delta^{18}O$, ‰ PDB	Sea Surface Temperature, °C
274	23.6	-	2.4
280	23.8	5.08	2.8
284	23.9	-	2.6
286	24.0	5.05	-
290	24.1	4.99	2.3
294	24.3	-	1.6
298	24.4	4.92	-
300	24.5	4.94	2.8
302	24.5	-	2.8
306	24.6	5.04	-
310	24.8	-	3.1
316	25.0	4.98	-
320	25.1	4.96	3.2
330	25.4	4.80	2.4
340	26.4	-	3.3
350	27.4	4.86	2.4
360	28.3	-	2.6
366	28.9	4.95	-
370	29.3	-	1.8
376	29.9	4.82	-
380	30.3	4.65	2.3
386	30.9	4.39	-
390	31.3	-	2.1
396	31.8	4.69	-
400	32.2	-	1.6
406	32.8	4.76	-
410	33.2	-	3.9
420	34.2	-	2.3
426	34.8	4.83	-
430	35.1	4.83	2.9
434	35.5	4.70	-
440	36.1	4.80	3.4
446	36.7	4.78	-
450	37.1	4.77	3.5
456	37.7	4.78	-
460	38.1	4.74	4.5
466	38.6	4.70	-
470	39.0	4.72	3.8
476	39.6	4.72	-
480	40.0	4.82	3.2
486	40.6	4.86	-
490	41.0	-	2.1
496	41.6	4.76	-
500	41.9	-	3.8
510	42.9	4.76	3.2
516	43.5	4.71	-
520	43.9	4.68	3.8
526	45.2	4.70	-
530	46.0	-	2.7
536	47.3	4.70	-
540	48.1	-	3.2

TABLE 3. (continued)

Sample Depth, cm	Age, ka	Benthic $\delta^{18}O$, ‰ PDB	Sea Surface Temperature, °C
550	50.2	4.60	3.4
556	50.6	4.64	-
560	50.9	4.63	5.5
570	51.5	-	2.8
580	52.2	4.66	2.6
590	52.8	4.72	2.1
600	53.5	4.68	3.7
610	54.1	-	2.4
616	54.5	4.74	-
620	54.8	4.52	4.4
626	55.2	4.71	-
630	55.5	4.60	4.2
640	56.0	4.60	4.4
644	56.3	-	5.1
646	56.4	4.66	-
650	56.6	-	2.9
652	56.7	-	3.0
656	57.0	4.70	-
660	57.2	-	5.4
670	57.8	4.62	3.3
680	58.4	4.70	4.9
690	59.0	4.71	2.1
696	64.1	4.86	-
700	68.8	4.74	3.4
704	69.6	-	4.0
710	70.8	4.89	2.8
714	71.2	-	1.7
716	71.4	4.74	3.0
720	71.7	4.54	1.2
726	72.2	4.44	-
730	72.6	4.56	1.1
736	73.1	4.68	-
740	73.5	4.53	1.6
750	74.4	4.40	3.2
754	74.8	-	2.9
760	75.4	4.19	1.8
762	75.6	-	1.7
764	75.8	-	1.7
766	76.0	-	4.0
768	76.1	-	3.1
770	76.3	4.29	3.1
774	76.7	-	2.6
780	77.3	4.32	7.7
784	77.7	-	2.2
790	78.3	4.32	6.1
794	78.7	-	3.9
798	79.1	-	6.3
800	79.3	4.21	8.7
802	79.8	-	8.5
808	81.6	-	8.0
810	82.2	4.18	7.4
814	83.4	-	6.8

TABLE 3. (continued)

Sample Depth, cm	Age, ka	Benthic $\delta^{18}O$, ‰ PDB	Sea Surface Temperature, °C
820	85.1	4.18	8.3
824	86.3	-	6.2
830	88.0	4.28	8.8
832	88.6	-	7.7
834	89.2	-	7.3
836	89.8	-	8.8
838	90.4	-	6.3
840	91.0	4.34	6.9
842	91.2	-	4.4
844	91.5	-	3.5
846	91.7	-	2.1
848	92.0	-	2.9
850	92.3	4.30	5.8
860	93.6	4.23	4.6
870	94.9	4.25	2.9
880	96.2	4.16	7.3
890	97.8	4.12	6.9
894	98.4	-	6.2
900	99.4	4.18	7.0
902	100.2	-	5.7
904	100.9	-	7.9
906	101.7	-	6.9
910	103.3	4.13	8.4
920	104.8	4.33	6.3
930	106.3	4.32	-
930	106.3	-	4.8
940	107.8	4.28	4.7
950	109.3	4.24	2.3
960	110.8	4.30	4.6
970	114.7	4.05	4.4
980	118.6	3.71	7.7
990	122.6	3.28	9.3
1000	125.2	3.38	8.2
1010	127.8	4.00	8.8
1020	130.3	4.64	7.2
1030	132.7	4.32	3.7
1040	135.1	5.02	3.2
1050	136.0	4.89	2.6
1060	136.9	5.00	2.8
1070	137.8	-	2.2
1080	138.7	4.94	3.6
1090	139.6	5.01	2.2
1100	140.5	4.91	3.2
1110	141.4	4.92	2.0
1120	142.3	4.75	3.6
1130	143.6	4.84	3.1
1140	144.9	4.86	3.1
1150	146.1	4.84	2.7
1160	147.4	4.86	3.8
1170	148.7	4.88	2.9
1180	150.0	-	2.9
1190	151.3	-	3.9

TABLE 3. (continued)

Sample Depth, cm	Age, ka	Benthic $\delta^{18}O$, ‰ PDB	Sea Surface Temperature, °C
1196	152.1	4.92	-
1200	152.6	-	3.1
1210	153.4	-	2.0
1220	154.2	-	1.5
1226	154.7	4.74	-
1230	155.0	-	1.5
1240	155.8	-	0.5
1250	156.6	4.43	-
1250	156.6	-	1.7
1256	157.0	4.58	-
1260	157.4	4.72	-
1260	157.4	-	1.5
1270	158.2	4.70	-
1270	158.2	-	1.9
1280	159.0	-	2.8
1290	159.7	-	1.7
1300	160.5	-	3.1

Ages are based on the correlation into the stacked SPECMAP $\delta^{18}O_{foram}$ record. The $\delta^{18}O_{foram}$ data is a composite record of the Cibicides and Uvigerina species. The last column lists the sea surface temperatures as deduced from the diatom transfer function D166/34/4 [Pichon et al., 1992]. PDB indicates Pee Dee belemnite.

CONCLUSIONS

We have constructed a record of $\delta^{18}O_{atm}$ from the analyses of trapped gases in the Vostok ice core covering the last full glacial cycle. Our $\delta^{18}O_{atm}$ record is very similar to the seawater $\delta^{18}O$ record over the same period. We interpret this strong similarity as an indication that changes in the $\delta^{18}O$ of seawater, which are known to be associated with changes in the volume of continental ice, have been transmitted to the atmospheric O_2 reservoir by photosynthesizing organisms near the surface of the ocean and on the continents. Furthermore, it appears that the major factor influencing $\delta^{18}O_{atm}$ is the $\delta^{18}O$ of seawater. Based on the similar behavior of these two $\delta^{18}O$ records, we have correlated the $\delta^{18}O_{atm}$ record from the Vostok ice core into the $\delta^{18}O_{foram}$ record from V19-30 using an inverse correlation method. Results of the correlation with eight coefficients show that 77% of the variance is shared between the $\delta^{18}O_{atm}$ and $\delta^{18}O_{sw}$ records.

We have utilized the results of the correlation to derive an ice age-depth relation for the Vostok ice core. The record of accumulation rate deduced from our correlated ice age-depth relation differs from that developed by Lorius et al. [1985]. For the correlated ice age-depth curve, the accumulation rate during the last glacial maximum and subsequent deglaciation is as much as 50% lower than that for the Lorius et al. [1985] age model. For the rest of the core, the correlated record of accumulation rate shows large oscillations which are most likely the result of 1- to 3-kyr errors in our ice age-depth relation. Such errors may result from errors in (1) the SPECMAP timescale which are calculated to lie between 1.1 and 7.7 kyr [Martinson et al., 1987], (2) estimates of Δage which are probably less than $\pm$ 2 kyr, and (3) estimates of the turnover time of atmospheric O_2 ($\pm$0.5 kyr). Errors may also result from the fact that $\delta^{18}O_{atm}$ can be influenced by hydrologic and biologic variability in addition to changes in $\delta^{18}O_{sw}$.

We have investigated the fidelity of the correlated ice age-depth relation by comparing a sea surface temperature record from the southern ocean with the record of Antarctic temperature from the Vostok ice core. The high degree of covariation between these two records supports the use of $\delta^{18}O_{atm}$ as a proxy for $\delta^{18}O_{sw}$ and indicates that our correlated age-depth curve for Vostok gives a chronology which is more consistent with the SPECMAP chronology.

Because of poor sample resolution between 400- and 800-m depth and the small changes in $\delta^{18}O_{sw}$ between 25 and 55 ka in the SPECMAP record, we are unable to reliably correlate the two $\delta^{18}O$ records over this time/depth interval.

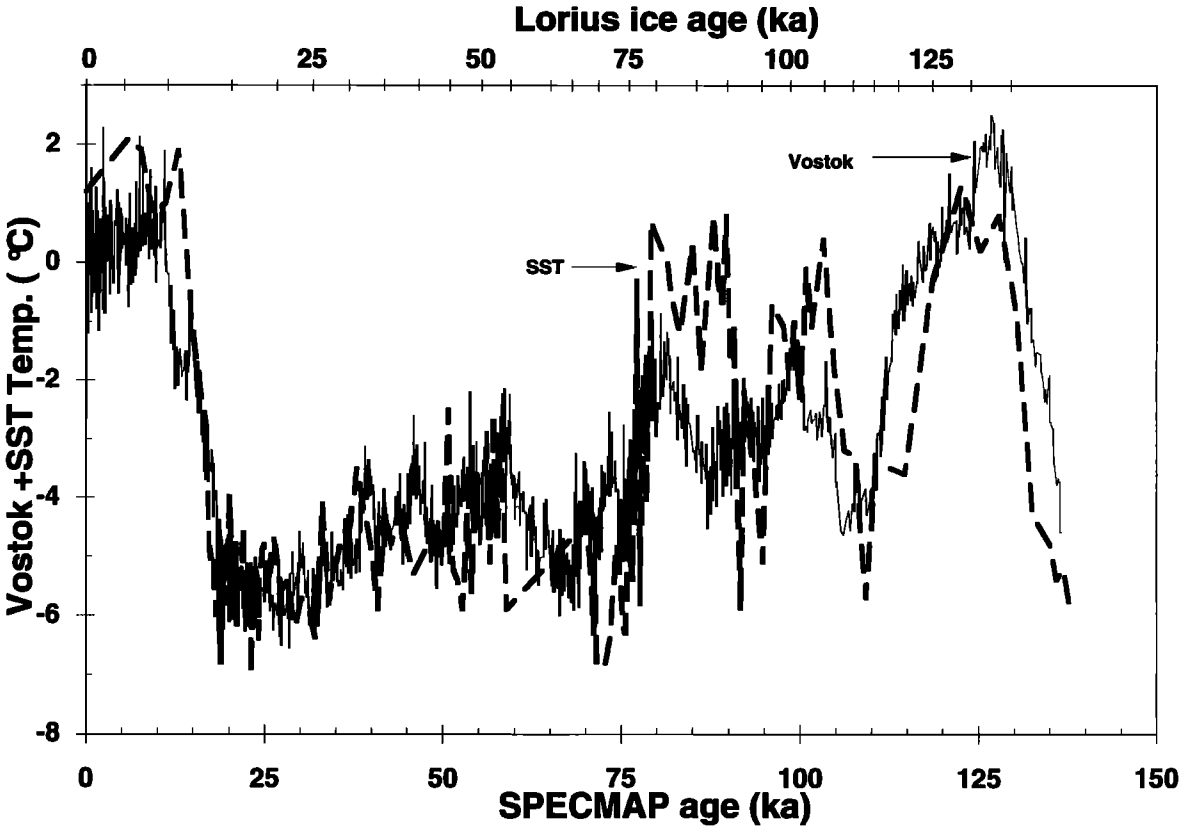

Fig. 8. Records of the Vostok inversion layer temperature and the sea surface temperature (SST) record from MD88-770 plotted on the common temporal framework. The age model for the Vostok inversion layer temperature is our best estimate from Figure 5. The SST record from MD88-770 has a stated uncertainty of ± 1°C. The plot shows a higher degree of similarity than a similar plot made with the Vostok temperature record plotted on the Lorius et al. [1985] chronology. We interpret this result as support for our common temporal framework and therefore our use of $\delta^{18}O_{atm}$ as a proxy for $\delta^{18}O_{sw}$. For reference, we have plotted the Lorius et al. [1985] timescale on the upper axis for comparison.

The data and arguments presented here do not give any reason to believe that our chronostratigraphy is any better or worse than that of Lorius et al. [1985]. Future efforts to date Greenland ice cores by counting annual dust layers back through the penultimate deglaciation will help in constructing absolute ice core chronologies. As these "absolute" chronologies become available, we will then be able to establish the relationship between the ice core climate records and any climate records which can be ^{230}Th - ^{234}U dated.

APPENDIX: CONSTRUCTING AN ICE AGE-DEPTH RELATIONSHIP FOR THE VOSTOK ICE CORE

We used the following approach to calculate an ice age-depth curve for the Vostok ice core.

1. Calculate the correlation gas age of each trapped gas sample in the Vostok ice core. The correlation age is our estimate of the gas age at each sample depth according to the SPECMAP chronology. It is calculated as described in an earlier section.

2. Calculate the ice age-gas age difference (Δage) for each sample using the densification approach outlined by Sowers et al. [1992]. Briefly, air is assumed to mix rapidly through the firn to the depth of bubble close-off. We assume that the density of ice in the bubble close off region increases with decreasing temperature according to the empirical relation of Martinerie et al. [1992]. The depth at which firn reaches this close off density is given as a function of accumulation rate and temperature by the empirical equations of Herron and Langway [1980]. The ice age at this depth is the ice age-gas age difference and equals the mass of the overburden per unit area divided by the mean accumulation rate.

This approach gives Δage values very close to those calculated using the method of Barnola et al. [1991].

3. Calculate the ice age at each depth by adding Δage (calculated in step 2) to the correlation gas age for each depth calculated in step 1.

4. Calculate ice accumulation rate as a function of depth. Accumulation rate is equal to the slope of the ice age-depth curve divided by the thinning function. The thinning function is defined as the mass per unit area of an annual layer of ice at depth z in the ice sheet divided by the mass per unit area at the time of deposition. For this calculation we have adopted the thinning function calculated by Ritz [1992].

5. Recalculate Δage values for each gas sample using the curve of accumulation rate versus depth calculated in step 4. The point of this recalculation is to estimate Δage values which are consistent with the correlated ice age depth relation.

6. Calculate another estimate of the ice age versus depth relation by adding the Δage values from step 5 to the correlated gas age at each depth from step 1.

7. Calculate the "correlation ice age versus depth" relation by averaging the ice ages from steps 3 and 6. We average the ice ages because the iterative procedure described above causes ice ages of some samples to diverge with successive iterations. Our ice age curves did not converge with successive iterations because of errors in the initial correlated gas age-depth relation which are on the order of a few centuries. These errors result in anomalous accumulation rate estimates, which lead to errors in subsequent Δage estimates over some portions of the core. We note that ice ages calculated in steps 3 and 6 differ by an average of 0.2 kyr, with a maximum difference of 2 kyr.

Does our chronology give reasonable curves of accumulation rate? One test of our curve of correlated ice age versus depth is whether or not it provides reasonable estimates of accumulation rate throughout the study period. In Figure 9, we plot

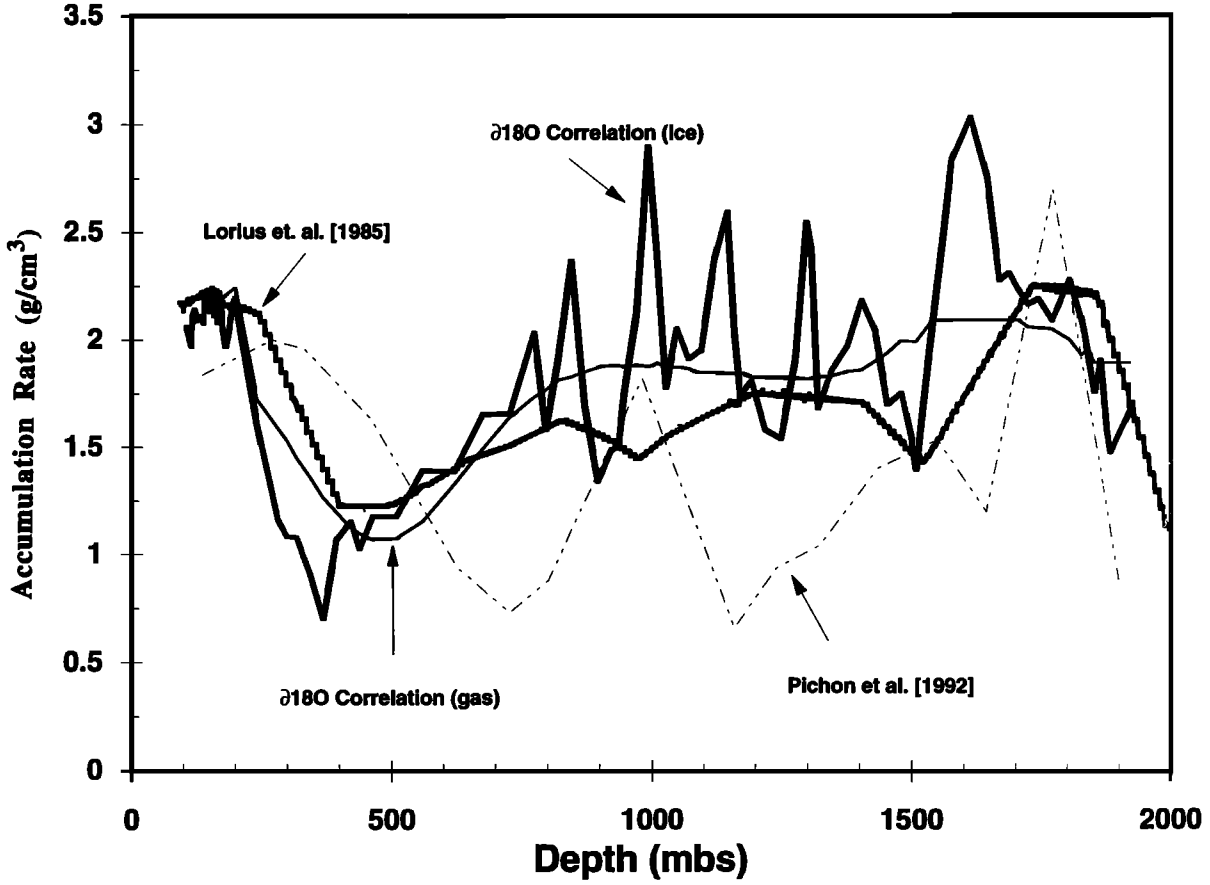

Fig. 9. Records of the surface accumulation rate at Vostok. The thick line is derived from the Lorius et al. [1985] ice age versus depth relation and has been corrected for thinning. The other three curves are from the $\delta^{18}O$ correlation (gas and ice) and the diatom correlation (dashed line). Note the lower accumulation rates calculated from the $\delta^{18}O$-correlated ice age-depth relations between 300 and 500 mbs. Also note the large oscillations in the correlated accumulation rate profile below 700 m below surface (mbs).

accumulation rate versus depth for all correlative age models for Vostok. For comparison, we also plot the record of accumulation rate of Lorius et al. [1985]. There are two curves from this study which are marked $\delta^{18}O$ correlation (ice) and $\delta^{18}O$ correlation (gas). The curve labeled $\delta^{18}O$ correlation (gas) is the derivative of the mapping function from the $\delta^{18}O$ of O_2 and $\delta^{18}O_{sw}$ correlation. The curve labeled $\delta^{18}O$ correlation (ice) is the slope of the correlation ice age versus depth relation described in the previous section. Our $\delta^{18}O$ correlation (ice) curve oscillates with a high frequency while the paleoaccumulation record from Lorius et al. [1985] varies slowly. We attribute much of the high-frequency oscillations to small errors in our age estimates.

The high-frequency variations in accumulation rates implied by our chronology (Figure 8) are glaciologically improbable. However, they do not imply large errors in estimated ages. Consider two levels within the core which have been assigned ice ages differing by 2 kyr. If the error in the relative ages of these levels is 1.0 kyr, then the accumulation rate calculated for the interval in question would be higher than the original value by a factor of 2 or lower by a factor of 0.67. This range of accumulation rates is comparable to the oscillations in the accumulation rate which we observe in Figure 9. We thus attribute a large portion of the difference between the two curves of accumulation rate shown in Figure 9 to uncertainties in the correlated ice age assigned to each depth. Dating errors could be the result of small errors in the SPECMAP chronology, uncertainties in calculated values of Δage, or variations in the M-D effect.

With our chronology, the depth interval between 290 and 360 m (termination I) corresponds to a period of 6 kyr, which is 2.8 kyr longer than that estimated using the flow model approach [Lorius et al., 1985]. The longer duration, inferred from our correlation, corresponds to accumulation rates which are 55% lower than those estimated by Lorius et al. [1985]. Accumulation rates for this depth interval from the Pichon et al. [1992] chronology are 25% higher than those inferred from the flow model.

Accumulation rate estimates from the flow model are consistent with ^{10}Be data for the Vostok ice core if one assumes that the flux of ^{10}Be to Vostok was about 38% higher during the last glacial maximum [Raisbeck et al., 1992]. There are three factors which influence the [^{10}Be] in ice at Vostok: (1) the production of ^{10}Be in the atmosphere (which is dictated by the flux of cosmic rays to the outer portion of the Earth's atmosphere and the intensity of the Earth's geomagnetic field), (2) the accumulation rate at the time of deposition, and (3) variations in local precipitation patterns on the East Antarctic plateau [Raisbeck et al., 1992]. We have estimated the flux of ^{10}Be to the Vostok area using the accumulation rate curves shown in Figure 9 and the Vostok [^{10}Be] record from [Raisbeck et al., 1992]. Our calculations indicate that the glacial ^{10}Be flux to Vostok was 19% higher for our correlated ice age depth relation, 38% higher for the Lorius age model, and 83% higher for the Pichon age model relative to Holocene values. These results are in qualitative agreement with the higher flux of ^{10}Be to the Pacific Ocean during the same time [Lao et al., 1992]. Furthermore, if we assume that the local precipitation patterns around Vostok remained constant over the last 25 ka, then the enhanced flux of ^{10}Be during glacial periods supports the hypothesis that ^{10}Be production was enhanced during the last glacial maximum.

Acknowledgments. We would like to thank all the members of the Soviet Antarctic Expeditions, Terres Australes et Antarctiques Françaises (TAAF), Expeditions Polaires Françaises (EPF), and the Office of Polar Programs (NSF) who helped retrieve and transport the Vostok core. J. Orchardo kindly provided his analytical expertise. We are also grateful to J. M. Barnola, E. Bard, C. Lorius, C. Ritz, J. Imbrie, and all the SPECMAP heroes for their useful comments. This research was supported on the American side by the NSF Division of Polar Programs (DPP grants 8820807 and 8822020) and on the French side by TAAF and Programme National d'Etude de la Dynamique du Climat. DGM's research was supported by NSF grant 8312637 (SPECMAP). This is Lamont-Doherty Earth Observatory contribution 5081.

REFERENCES

Bard, E., B. Hamelin, R. Fairbanks, and A. Zindler, Calibration of the ^{14}C timescale over the past 30,000 years using mass spectrometric U-Th ages from Barbados corals, *Nature, 345*, 405-410, 1990*a*.

Bard, E., B. Hamelin, and R. G. Fairbanks, U-Th ages obtained by mass spectrometry in corals from Barbados: Sea level during the past 130,000 years, *Nature, 346*, 456-458, 1990*b*.

Barnola, J. M., D. Raynaud, Y. S. Korotkevich, and C. Lorius, Vostok ice core provides 160,000-year record of atmospheric CO_2, *Nature, 329*, 408-414, 1987.

Barnola, J. M., P. Pimienta, D. Raynaud, and Y. S. Korotkevich, CO_2-climate relationship as deduced from the Vostok ice core: A reexamination based on new measurements and on a reevaluation of the air dating, *Tellus, Ser. B, 43*, 83-90, 1991.

Beer, J., S. J. Johnsen, G. Bonnani, R. C. Finkel, C. C. Langway, H. Oeschger, B. Stauffer, M. Suter, and W. Woelfli, ^{10}Be peaks as time markers in polar ice cores, in *The Last Deglaciation: Absolute and Radiocarbon Chronologies,* edited by E. Bard and W.

Broecker, pp. 141-153, Springer-Verlag, New York, 1992.

Bender, M. L., L. D. Labeyrie, D. Raynaud, and C. Lorius, Isotopic composition of atmospheric O_2 in ice linked with deglaciation and global primary productivity, *Nature, 318*, 349-352, 1985.

Birchfield, G. E., Changes in deep-ocean water $\delta^{18}O$ and temperature from the last glacial maximum to the present, *Paleoceanography, 2*, 431-442, 1987.

Chappell, J., and N. J. Shackleton, Oxygen isotopes and sea level, *Nature, 324*, 137-140, 1986.

Chappellaz, J., J.-M. Barnola, D. Raynaud, Y. S. Korotkevich, and C. Lorius, Atmospheric CH_4 record over the last climatic cycle revealed by the Vostok ice core, *Nature, 345*, 127-131, 1990.

Craig, H., Y. Horibe, and T. A. Sowers, Gravitational separation of gases and isotopes in polar ice caps, *Science, 242*, 1675-1678, 1988.

Dansgaard, W., H. B. Clausen, N. Gundestrup, S. J. Johnsen, and C. Rygner, Dating and climatic interpretation of two deep Greenland ice cores, in *Greenland Ice Core: Geophysics, Geochemistry, and the Environment, Geophys. Monogr. Ser.*, Vol. 33, edited by C. C. Langway Jr., et al., pp. 71-76, AGU, Washington, D.C., 1985.

Dole, M., The relative atomic weight of oxygen in water and air, *J. Am. Chem. Soc., 57*, 2731-2732, 1935.

Dole, M., G. A. Lane, D. P. Rudd, and D. A. Zaukelies, Isotopic composition of atmospheric oxygen and nitrogen, *Geochim. Cosmochem. Acta., 6*, 65-78, 1954.

Etheridge, D., G. Pearman, and P. Fraser, Changes in tropospheric methane between 1841 and 1978 from a high accumulation rate Antarctic ice core, *Tellus, Ser. B, 44*, 282-294, 1992.

Fairbanks, R. G., and R. K. Matthews, The marine oxygen isotope record in Pleistocene coral, Barbados, West Indies, *Quat. Res. N. Y., 10*, 181-196, 1978.

Guiot, J., A. Pons, J. L. de Beaulieu, and M. Reille, A 140,000-year continental climate reconstruction from two European pollen records, *Nature, 338*, 309-313, 1989.

Hammer, C. U., H. B. Clausen, and H. Tauber, Ice-core dating of the Pleistocene/Holocene boundary applied to a calibration of the ^{14}C time scale, *Radiocarbon, 28*, 284-291, 1986.

Hays, J. D., J. Imbrie, and N. J. Shackleton, Variations in the Earth's orbit: Pacemaker of the ice ages, *Science, 194*, 1121-1132, 1976*a*.

Hays, J. D., J. Lozano, N. Shackleton, and G. Irving, Reconstruction of the Atlantic and Western Indian Ocean sectors of the 18,000 B. P. Antarctic Ocean, in *Investigation of Late Quaternary Paleoceanography and Paleoclimatology*, edited by R. M. Cline, pp. 337-372, Geological Society of America, Boulder, Colo., 1976*b*.

Herron, M. M., and C. C. Langway, Jr., Firn densification: An empirical model, *J. Glaciol., 25*, 373-385, 1980.

Hovan, S. A., D. K. Rea, and N. G. Pisias, Late Pleistocene continental climate and oceanic variability recorded in northwest Pacific sediments, *Paleoceanography, 6*, 349-370, 1991.

Howard, W. R., and W. L. Prell, Late Quaternary surface circulation of the Southern Indian Ocean and its relationship to orbital variations, *Paleoceanography, 7*, 79-118, 1992.

Imbrie, J., J. D. Hays, D. G. Martinson, A. McIntyre, A. C. Mix, J. J. Morley, N. G. Pisias, W. L. Prell, and N. J. Shackleton, The orbital theory of Pleistocene climate: Support from a revised chronology of the marine $\delta^{18}O$ record, in *Milankovitch and Climate*, edited by A. Berger et al., pp. 269-305, D. Reidel, Norwell, Mass., 1984.

Johnsen, S. J., H. B. Clausen, W. Dansgaard, K. Fuhrer, N. Gundestrup, C. U. Hammer, P. Iversen, J. Jouzel, B. Stauffer, and J. P. Steffensen, Irregular glacial interstadials recorded in a new Greenland ice core, *Nature, 359*, 311-313, 1992.

Jouzel, J., and L. Merlivat, Deuterium and oxygen 18 in precipitation: Modeling of the isotopic effects during snow formation, *J. Geophys. Res., 89*, 11,749-11,757, 1984.

Jouzel, J., C. Lorius, J. R. Petit, C. Genthon, N. I. Barkov, V. M. Kotlyakov, and V. M. Petrov, Vostok ice core: a continuous isotope temperature record over the last climatic cycle (160,000 years), *Nature, 329*, 403-407, 1987.

Jouzel, J., G. Raisbeck, J. P. Benoist, F. Yiou, C. Lorius, D. Raynaud, J. R. Petit, N. I. Barkov, Y. S. Korotkevitch, and V. M. Kotlyakov, A comparison of deep Antarctic ice cores and their implications for climate between 65,000 and 15,000 years ago, *Quat. Res. N.Y., 31*, 135-150, 1989.

Jouzel, J., J. R. Petit, N. I. Barkov, J. M. Barnola, J. Chappellaz, P. Ciais, v. M. Kotkyakov, C. Lorius, V. N. Petrov, D. Raynaud, and C. Ritz, The last deglaciation in Antarctica: Further evidence of a "Younger Dryas" type climatic event., in *The Last Deglaciation: Absolute and Radiocarbon Chronologies*, edited by E. Bard and W. Broecker, pp. 229-266, Springer-Verlag, New York, 1992.

Jouzel, J., N. I. Barkov, J. M. Barnola, M. Bender, J. Chappellaz, C. Genthon, V. M. Kotlyakov, V. Lipenkov, C. Lorius, J. R. Petit, D. Raynaud, G. Raisbeck, C. Ritz, T. Sowers, M. Stievenard, F. Yiou, and P. Yiou, Vostok ice cores: extending the climatic records over the penultimate glacial period, *Nature, 364*, 407-412, 1993.

Kotlyakov, V. M., Global changes over the last climatic cycle from Antarctic ice core records, in *Glaciers-Ocean-Atmosphere Interactions*, edited by V. M. Kotlyakkov, pp. 15-27, International

Association of Hydrological Sciences, St. Petersburg, Russia, 1990.
Kroopnick, P., and H. Craig, Atmospheric oxygen: Isotopic composition and solubility fractionation, *Science, 175*, 54-55, 1972.
Kukla, G., and Z. A. An, Loess stratigraphy in central China, *Palaeogeogr. Palaeoclimatol. Palaeoecol., 72*, 203-225, 1989.
Labeyrie, L. D., J. C. Duplessy, and P. L. Blanc, Variations in mode of formation and temperature of oceanic deep waters over the past 125,000 years, *Nature, 327*, 477-482, 1987.
Lambeck, K., and M. Nakada, Constraints on the age and duration of the last interglacial period and on sea -level variations, *Nature, 357*, 125-128, 1992.
Lao, Y., R. F. Anderson, W. S. Broecker, S. E. Trumbore, F. J. Hofmann, and W. Wolfli, Increased production of cosmogenic ^{10}Be during the last glacial maximum, *Nature, 357*, 576-578, 1992.
Lorius, C., J. Jouzel, C. Ritz, L. Merlivat, N. E. Barkov, and Y. S. Korotkevich, A 150,000-year climatic record from Antarctic ice, *Nature, 316*, 591-595, 1985.
Lozano, J., and J. D. Hays, Relationship of radiolarian assemblages to sediment types and physical oceanography in the Atlantic and Western Indian ocean sectors of the Antarctic Ocean, in *Investigation of Late Quaternary Paleoceanography and Paleoclimatology,* edited by J. D. Hays, pp. 303-336, Geological Society of America, Boulder, Colo., 1976.
Lyle, M., Climatically forced organic carbon burial in equatorial Atlantic and Pacific oceans, *Nature, 335*, 529-532, 1988.
Martinerie, P., D. Raynaud, D. Etheridge, J.-M. Barnola, and D. Mazaudier, Physical and climatic parameters which influence the air content in polar ice, *Earth Planet. Sci. Lett., 112*, 1-13, 1992.
Martinson, D. G., W. Menke, and P. Stoffa, An inverse approach to signal correlation, *J. Geophys. Res., 87*, 4807-4818, 1982.
Martinson, D. G., N. G. Pisias, J. D. Hays, J. Imbrie, T. C. Moore Jr., and N. J. Shackleton, Age dating and the orbital theory of the ice ages: development of a high-resolution 0 to 300,000-year chronostratigraphy, *Quat. Res. N.Y., 27*, 1-27, 1987.
Meyer, M. K., Net primary productivity estimates for the last 18,000 years evaluated from simulations by a global climate model, M. S. thesis, Univ. of Wisconsin, Madison, 1988.
Mix, A. C., Influence of productivity variations on long-term atmospheric CO_2, *Nature, 337*, 541-544, 1989.
Morita, N., The increased density of air oxygen relative to water oxygen, *Nippon Kagaku Kaishi, 56*, 1291, 1935.
Neftel, A., H. Oeschger, T. Staffelbach, and B. Stauffer, CO_2 record in the Byrd ice core 50,000-5,000 years BP, *Nature, 331*, 609-611, 1988.
Petit, J. R., L. Mounier, J. Jouzel, Y. S. Korotkevich, V. I. Kotlyakov, and C. Lorius, Paleoclimatological and chronological implications of the Vostok core dust record, *Nature, 343*, 56-58, 1990.
Phillpot, H. R., and J. W. Zillman, The surface temperature inversion over the Antarctic continent, *J. Geophys. Res., 75*, 4161-4169, 1970.
Pichon, J.-J., L. D. Labeyrie, G. Bareille, M. Labracherie, J. Durpat, and J. Jouzel, Surface water temperature changes in the high latitudes of the southern hemisphere over the last glacial-interglacial cycle, *Paleoceanography, 7*, 289-318, 1992.
Pisias, N. G., D. G. Martinson, T. C. Moore, N. J. Shackleton, W. Prell, and B. Boden, High resolution stratigraphic correlation of benthic oxygen isotopic records spanning the last 300,000 years, *Mar. Geol., 56*, 119-136, 1984.
Prell, W. L., and J. E. Kutzbach, Monsoon variability over the past 150,000 years, *J. Geophys. Res., 92*, 8411-8425, 1987.
Prell, W. L., J. Imbrie, D. G. Martinson, J. J. Morley, N. G. Pisias, N. J. Shackleton, and H. F. Streeter, Graphic correlation of oxygen isotope stratigraphy: Application to the late Quaternary, *Paleoceanography, 1*, 137-162, 1986.
Raisbeck, G. M., F. Yiou, D. Bourles, C. Lorius, J. Jouzel, and N. I. Barkov, Evidence for two intervals of enhanced ^{10}Be deposition in Antarctic ice during the last glacial period, *Nature, 326*, 273-277, 1987.
Raisbeck, G. M., F. Yiou, J. Jouzel, J. R. Petit, N. I. Barkov, and E. Bard, ^{10}Be deposition at Vostok, Antarctica during the last 50,000 years and its relationship to possible cosmogenic production variations during this period, in *The Last Deglaciation: Absolute and Radiocarbon Chronologies,* edited by E. Bard and W. Broecker, pp. 125-139, Springer-Verlag, New York, 1992.
Raynaud, D., J. Chappellaz, J.-M. Barnola, Y. S. Korotkevich, and C. Lorius, Climatic and CH_4 cycle implications of glacial-interglacial CH_4 change in the Vostok ice core, *Nature, 333*, 655-657, 1988.
Reeh, N., S. J. Johnsen, and D. Dahl-Jensen, Dating the Dye 3 deep ice core by flow model Calculations, in *Greenland Ice Core: Geophysics, Geochemistry, and the Environment, Geophys. Monogr. Ser.,* Vol. 33, edited by C. C. Langway Jr., et al., pp. 71-76, AGU, Washington, D.C., 1985.
Ritz, C., Flow modeling the Vostok region, Ph. D. dissertation, Domaine Univ., Grenoble, France, 1992.

Robin, G. D. Q., Ice cores and climatic changes, *Philos. Trans.R. Soc. London, Ser. B, 280*, 143-168, 1977.

Sarnthein, M., E. Jansen, M. Arnold, J. C. Duplessy, H. Erienkeuser, A. Flatoy, T. Veum, E. Vogelsang, and M. S. Weinelt, $\delta^{18}O$ time-slice reconstruction of meltwater anomalies at termination I in the North Atlantic between 50 and 80°N, in *The Last Deglaciation: Absolute and Radiocarbon Chronologies,* edited by E. Bard and W. S. Broecker, pp. 183-200, Springer-Verlag, New York, 1992.

Schwander, J., The transformation of snow to ice and the occlusion of gases, in *The Environmental Record in Glaciers and Ice Sheets,* edited by H. Oeschger and C. C. Langway, pp. 53-67, John Wiley, New York, 1989.

Shackleton, N. J., Oxygen isotopes, ice volume and sea level, *Quat. Sci. Rev., 6*, 183-190, 1987.

Shackleton, N. J., and N. D. Opdyke, Oxygen isotope and paleomagnetic stratigraphy of equatorial Pacific core V28-238: Oxygen isotope temperatures and ice volumes on a 10^5 and 10^6 year scale, *Quat. Res. N. Y., 3*, 39-55, 1973.

Shackleton, N. J., and N. G. Pisias, Atmospheric carbon dioxide, orbital forcing , and climate, in *The Carbon Cycle and Atmospheric CO_2 Natural Variations Archean to Present, Geophys. Monogr. Ser., vol. 32,* edited by E. T. Sundquist and W. S. Broecker, pp. 303-317, AGU, Washington, DC, 1985.

Shackleton, N., J. Le, A. Mix, and M. A. Hall, Carbon isotope records from Pacific surface waters and atmospheric carbon dioxide, *Quat. Sci. Rev., 11*, 387-400, 1992.

Sowers, T. A., M. L. Bender, and D. Raynaud, Elemental and isotopic composition of occluded O_2 and N_2 in polar ice, *J. Geophys. Res., 94*, 5137-5150, 1989.

Sowers, T., M. Bender, D. Raynaud, Y. S. Korotkevich, and J. Orchardo, The $\delta^{18}O$ of atmospheric O_2 from air inclusions in the Vostok ice core: Timing of CO_2 and ice volume changes during the penultimate deglaciation, *Paleoceanography, 6*, 679-696, 1991.

Sowers, T., M. Bender, D. Raynaud, and Y. S. Korotkevich, The $\delta^{15}N$ of N_2 in air trapped in polar ice: A tracer of gas transport in the firn and a possible constraint on ice age-gas age differences, *J. of Geophys. Res., 97*, 15,683-15,697, 1992.

Stauffer, B., E. Lochbronner, H. Oeschger, and J. Schwander, Methane concentration in the glacial atmosphere was only half that of the preindustrial Holocene, *Nature, 332*, 812-814, 1988.

Yiou, F., G. M. Raisbeck, D. Bourles, C. Lorius, and N. I. Barkov, ^{10}Be in ice at Vostok Antarctica during the last climatic cycle, *Nature, 316*, 616-617, 1985.

M. Bender and T. Sowers, Graduate School of Oceanography, University of Rhode Island, Narragansett, RI 02882-1197.

J. Jouzel, Laboratoire de Modelisation du Climat et de l'Environnement Batiment 709, Orme des Meriseeirs, CE Saclay 91191 Gif Sur Yvette Cedex, France.

Y. S. Korotkevich, Arctic and Antarctic Research Institute Beringa Street 38, St. Petersburg, Russia.

L. Labeyrie, Centre des Faibles Radioactivites Laboratorie Mixte CNRS-CEA Parc du CNRS 91190 Gif Sur Yvette, France.

D. Martinson, Lamont-Doherty Earth Observatory Palisades, NY 10964.

J. J. Pichon, Department Géologie et Océanologie, URA 197, Av des Facultés Université Bordeaux 1, 33405 Talence Cedex France.

D. Raynaud, Laboratoire de Glaciologie et Geophysique de l'Environnement BP 96-38402 St. Martin d'Heres Cedex, France.

(Received January 14, 1993;
revised June 17, 1993;
accepted August 17, 1993.)